THE ASEAN JOURNAL OF RADIOLOGY

May-August 2012
Volume XVIII Number II
ISSN 0859 144X

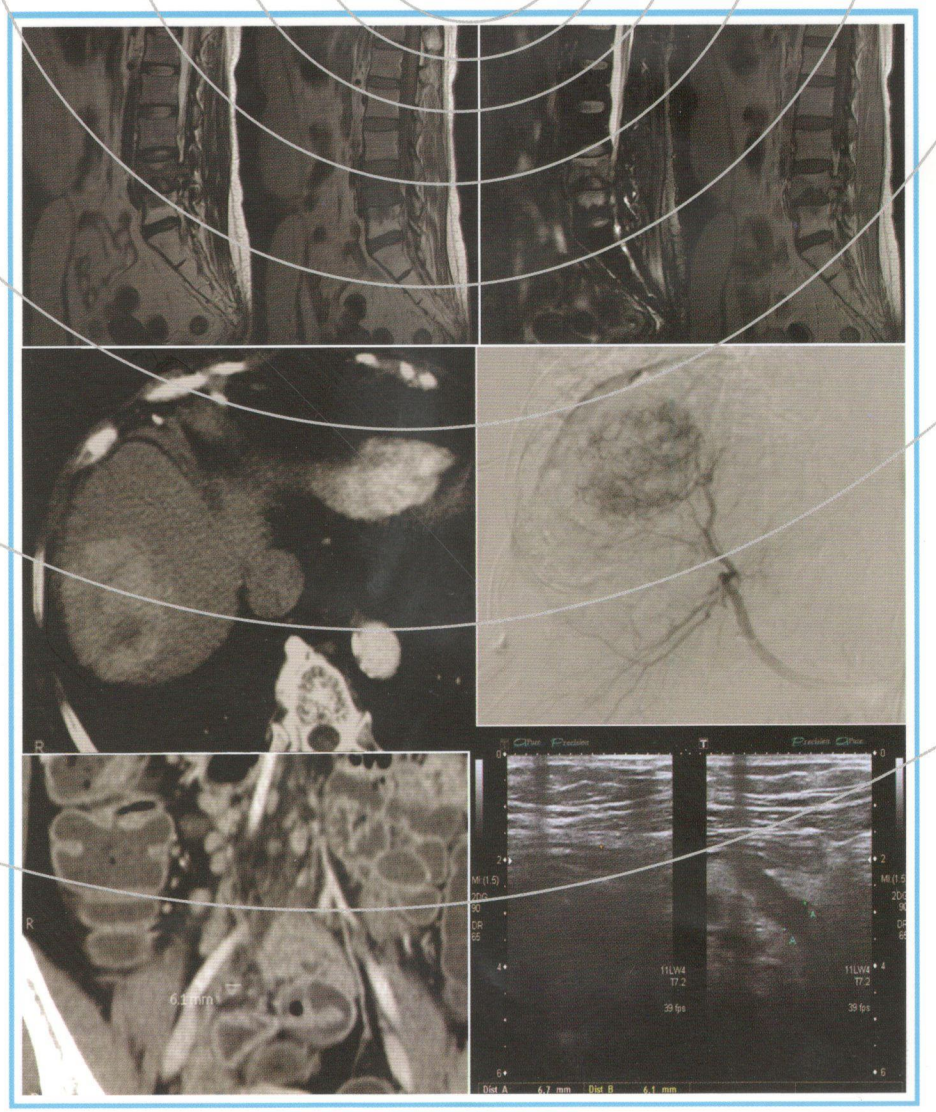

Published by

Royal College of Radiologists of Thailand

and

Radiological Society of Thailand

Bangkok, Thailand.

THE ASEAN JOURNAL OF RADIOLOGY
May-August 2012, Volume XVIII No.II

The Committee of Royal College of Radiologists of Thailand

Apr 2011-Mar 2013

President:	Permyot	Kosolbhand
Vice-president:	Sirintara	Singhara Na Ayudya
Secretariat General:	Pongdej	Pongsuwan
Vice-secretary General:	Alongkorn	Kiatdilokrath
Treasurer:	Krisdee	Prabhassawat
Academic president:	Anchalee	Churojana
House Master & Social Programme:	Kiat	Arjhansiri
Secretary:	Vithya	Varavithya
Registrar:	Pisit	Wattanaruangkowit
Committee:	Poonsook	Jitnuson
	Chamaree	Chuapatcharasopon
	Chantima	Rongviriyapanich
	Nitra	Piyaviseipat

The Committee of Radiological Society of Thailand

Apr 2011-Mar 2013

President:	Permyot	Kosolbhand
Vice-president:	Sirintara	Singhara Na Ayudya
Secretariat General:	Pongdej	Pongsuwan
Treasurer:	Krisdee	Prabhassawat
Academic president:	Anchalee	Churojana
House Master&Social Programme:	Kiat	Arjhansiri
Committee:	Poonsook	Jitnuson
	Chamaree	Chuapatcharasopon
	Chantima	Rongviriyapanich
	Nitra	Piyaviseipat
	Amphai	Uraiverotchanakorn

The Journal of the Royal College of Radiologists & Radiological Society of Thailand

(2011 - 2013)

Office:

1. Department of Radiology, Faculty of medicine, Ramathibodi hospital 270, Rama VI Road, Toong Phayathai, Ratchathewi, Bangkok, 10400
   Tel 02-2011259#110, Fax 02-2011297
   E-mail Sirintarapongpech2@hotmail.com

2. The Royal college of Radiologists & Radiological society of Thailand. 9th Floor, Royal Golden Jubilee Building, 2 Soi Soonvijai, Petchburi Road, Bankok, 10320
   Tel 02-7165963, Fax 02-7165964
   E-mail rcrtthailand@gmail.com

Contents

Original Article

THE ASEAN JOURNAL OF RADIOLOGY 2012: 18(2): 79-84 79

Original Article

The Effect of Zinc Amino Acid Chelate on Decrease of Taste Dysfunction in Head and Neck Cancer Patients After Complete Radiotherapy within 6 Months, A Prospective Randomized Controlled Trial

Kanograt Tangsriwong, Montien Pesee, Srichai Krusun, Vorachai Tangvoraphonkchai, Chunsri Supaadirek, Komsan Thamronganantasakul, Narudom Supakalin, Prawat Padoongcharoen

Division of Radiotherapy, Radiology department, Faculty of Medicine, Khon Kaen University, Thailand, 40002

Abstract

Objectives: To prospectively investigate whether Zinc amino acid chelate on decrease of taste dysfunction after complete radiotherapy within 6 months for improving taste ability in head and neck cancer patients treated with radiotherapy alone or concurrent chemoradiotherapy during radiotherapy.

Material and Methods: Between September 2010 and Febrauary 2012. Sixty-three patients were randomized to receive either Zinc or no Zinc administration, 31 patients received Zinc amino acid chelate and 32 patients without amino acid chelate administration. There were 42 evaluable patients which 2 cases were withdrawn and 19 cases loss to follow up.

Results: The study demonstrated no statistically significant on taste function after radiation completed within 1-6 months, with the sweet tastes (p=0.43), salty tastes (p=0.68) and sour tastes (p=0.51) between the patients received with Zinc amino acid chelate and without Zinc amino acid chelate administration.

Conclusion: All of the taste evaluations revealed no statistical significance between the patients received with Zinc amino acid chelate and without Zinc administration (p >0.05). The relatively small number of subjects in this study may contribute to the lack of statistical differences between groups.

Keywords: Zinc amino acid chelate, radiotherapy, taste dysfunction

Introduction

Adverse reactions of radiotherapy depend on area being irradiated, amount of total dose & fractionation, patient's age and underlying diseases. Acute reactions during treatment can be divided into early *(mucosa, taste, salivary glands)*, intermediate *(taste, salivary glands)*, and late *(salivary glands, dentition, periodontium, bone, muscles, joints)* effects. Complications occur in early phase could be cured whereas late complications are normally irreversible and leading to permanent incapability and poor quality of life[1,2]

Dysgeusia is one of complications that affects patients from the second or third week of radiotherapy and may last for several weeks or even months. Conger AD found that taste sensation decreased exponentially with a cumulative dose of 30 Gy, approximately, during the third week[3]. Then taste sensation becomes temporarily absent and no more loss occurred if no irradiation added. Apart from their radiosensitive properties, taste buds also decrease with the degeneration of their normal histological architecture from day 6-7 of irradiation. Major cause of taste perception loss is the direct effect of irradiation on taste buds and their cultured nerves. Alteration of salivary flow viscosity and saliva biochemical creates a physical barrier of saliva between tongue and foodstuff. Taste perception, therefore becomes worse which affects chewing and appetite as well. Destroyed taste buds also have effect on patients' unpalatable taste which will need approximately 6 months for treatment. Inokuchi found that salivary viscosity dysfunction was not likely the major factor affecting taste disturbance. The recovery period of taste buds generally takes place around 2-4 months or till 1 year after radiation completed. The degree of taste recovery and the recovery time depend on the radiation dose received[2].

Prevention of taste loss can be accomplished through direct shielding of healthy tissue or placement of these tissues outside the radiation field by shielding or repositioning prostheses. Treatment of taste dysfunction by cytoprotective drugs during irradiation could not be concluded[4,5]. Another means to treat patients with taste abnormalities is the use of Zinc element which is a cofactor in alkaline phosphatase enzyme, mostly found in taste bud cells membrane. The enzyme will control the quantity of stimuli which passing through pores for the perception. Zinc, therefore, brings taste perception and taste bud anatomy back to normal situation[6].

However, there are still no research or study of the effect of zinc amino acid chelate on taste dysfunction after radiotherapy in Thailand. This randomized controlled trial was therefore conducted to determine whether the effect of Zinc amino acid chelate on decrease of taste dysfunction in head and neck cancer patients treatment with radiotherapy alone or concurrent chemoradiotherapy after radiotherapy within 6 months.

Materials and Methods

This prospective randomized controlled trial was performed at Division of Radiotherapy, Department of Radiology, Faculty of Medicine, Khon Kaen University, Thailand, between September 2010 and February 2012. Sixty-three patients were randomized to receive either Zinc or no Zinc administration, 31 patients received Zinc amino acid chelate and 32 patients without amino acid chelate administration. There were 42 evaluable patients which 2 cases were withdrawn and 19 cases loss to follow up.

Inclusion criteria were (1) head and neck cancer

patients treated with radiotherapy covering the mouth. (2) age 20 to 70 years. Exclusion criteria were (1) had undergone surgery of the tongue. (2) receiving drug cytoprotective agent, captopril, penicillamine and metronidazole. (3) treated with head and neck irradiation and dosage below 50 Gy. (4) who had undergone surgery on organs of the smell associated with taste. (5) pregnant or during lactation. (6) history of oral contraceptives therapy. (7) who are dementia. This project has been approved by the Human Ethics Committee of Khon Kaen University (HE 531446).

The statistical analysis was performed by using the STATA software version 10.0 and SPSS software version 13. A *p*- value of less than 0.05 was considered statistically significant. Sex, smoke, alcohol drinking, favorite taste, diagnosis, radiotherapy technique and concentration of substances were described by Chi-Square. The results of taste test were calculated by Repeated-measures ANOVA method.

The patients were randomized by using simple random sampling to receive either Zinc amino acid chelate or non- Zinc amino acid chelate administration. The patients received doctor's explanation and also signed consent for research participation. (a) Both groups of the patients were evaluated the baseline taste function before radiotherapy, at 50 Gy of radiation and after complete radiotherapy within 1-6 months by using taste substances and concentration followed by Yamashita H, et al[9]. (b) Patients in experimental group were received Zinc amino acid chealate 15 mg once daily with irradiation or radiochemotherapy from the first day of start irradiation until completion of radiotherapy. The patients in control group were treated with irradiation or radiochemotherapy without Zinc administration. (c) This study used sucrose to test sweet. These substances used in liquid form and tested by a drop on the papilla from lowest to highest concentration and recorded minimum concentration that patients can distinguish the taste. (d) The sodium chloride was used to test salty, same as sweet test but will drop down almost to the front side of the tongue, either side. (e) The tartaric acid was used for sour test as sweet test but will drop down the side almost to the back of the tongue, another side of tongue for salty taste evaluation.(f) Participants will gargle before the taste evaluation next time. The measure used score 0-4 compared to Subjective Total Taste Acuity (STTA) scale[4]. (g) Test all the irradiated patients after radiation completed in the duration of 1-6 months in both groups. The score were recorded form of visual analog scale. (h) In order to measure of each flavor, the patients rated score by themselves and viewed the past score.

Results

Patient characteristics are summarized in Table 1, the diagnosis of disease in Table 2, the radiation techniques in Table 3, and taste evaluations in Table 4.

The analysis of taste function after radiation completed within 1-6 months revealed no statistical significance, with the sweet tastes (p=0.43), salty tastes (p=0.68) and sour tastes (p=0.51) between the patients received with Zinc amino acid chelate and without Zinc amino acid chelate administration.

The multivariate analysis of concurrent chemo-radiation or radiation alone and with or without Zinc amino acid chelate administration found that no statistical significance between the patients received with Zinc and without Zinc administration in all of the tastes; sweet taste (p=0.25), salty taste (p=0.56)

Table 1 Patients Characteristics

	Characteristic	Zinc (N=23)	No zinc (N=19)	Total (N=42)	%	*p*-value
Sex	Male	14	13	27	64.29	0.61
	Female	9	6	15	35.71	
Age	≤60 years old	14	23	37	88.10	0.09
	>60 years old	5	2	7	16.67	
Smoke	Yes	7	6	13	30.95	0.94
	No	16	13	29	69.05	
Drink	Yes	5	7	12	28.57	0.28
	No	18	12	30	71.43	

Table 2 The diagnosis of patients

Diagnosis	Zinc (N=23)	No zinc (N=19)	Total (N=42)	%	*p*-value
Oropharyngeal carcinoma	1	1	2	4.7	0.54
Base of tongue carcinoma	1	2	3	7.14	
Parotid gland carcinoma	1	2	3	7.14	
Nasopharygeal carcinoma	9	6	15	35.7	
Oral tongue carcinoma	3	3	6	14.29	
Maxillar and nasal cavity carcinoma	1	0	1	2.38	
Oral cavity carcinoma	4	2	6	14.29	
Hypopharyngeal carcinoma	2	1	3	7.14	
Diffuse large B cell lymphoma	0	1	1	2.38	

Table 3 Modalities of therapy and radiation techniques

		Zinc (N=23)	No zinc (N=19)	Total (N=42)	%	p-value
Volume of tongue	Partial tongue irradiation	9	10	19	45.24	0.38
	Whole tongue irradiation	14	9	23	54.76	
Technique	2D conventional irradiation	22	19	41	97.6	0.27
	3D conformal irradiation	1	0	1	2.4	
CCRT	Yes	15	13	28	66.67	0.83
	No	8	6	14	33.33	

Table 4 Taste evaluations at 50 Gy (A) and after complete radiation (B)

Tastes \ Thresholds		Minimum (score)	Maximum (score)	Mean (score)
Sweet	A	0	4	1.64
	B	0	4	2.62
Salt	A	0	4	1.57
	B	0	4	2.43
Sour	A	0	4	1.90
	B	0	4	2.95

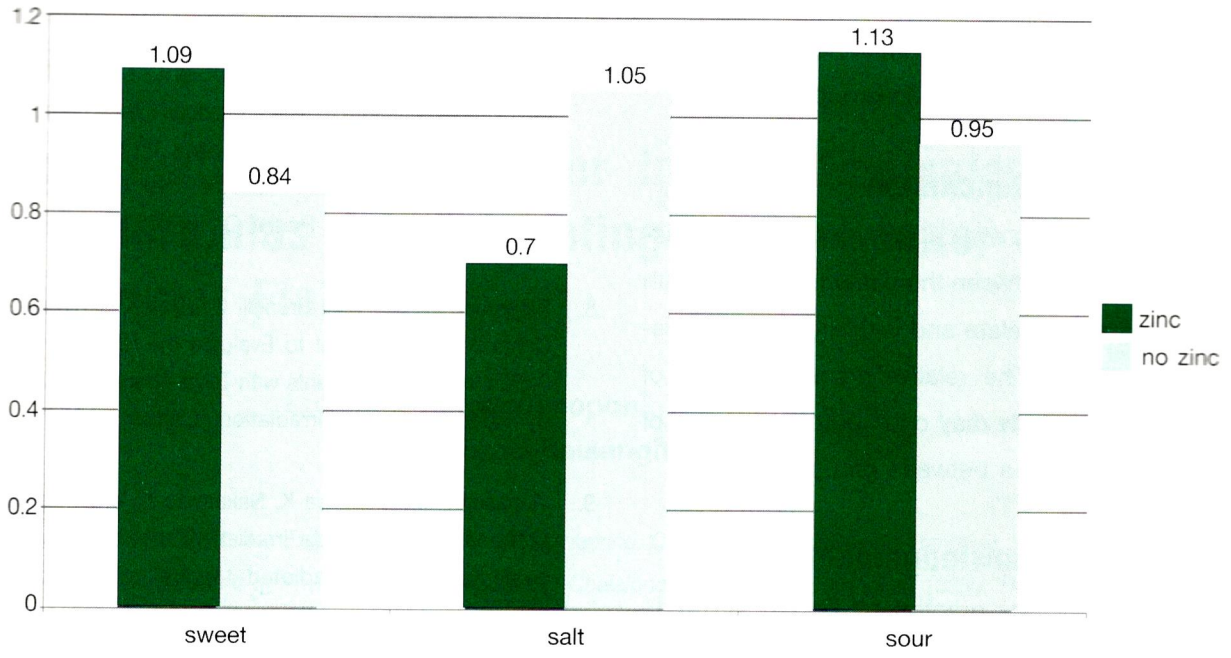

Fig.1 The mean difference of taste evaluation with or without Zinc amino acid chelate administration from the time of 50 Gy to 1-6 months after complete radiation

and sour taste (p=1.00). The analysis of partial and whole tongue irradiation with or without Zinc amino acid chelate administration found that no statistical significance in both groups; sweet taste (p=0.39), salty taste (p=0.56) and sour taste (p=1.00).

Discussion

Halyard et al.[7] evaluated taste alterations in 169 head and neck cancer patients who undergo radiotherapy with Zinc sulfate administration versus placebo. Taste acuity were assessed weekly during RT and at 1, 2, 3, 6 months after RT completion. The study revealed that Zinc sulfate did not decrease the incidence of taste alterations and taste recovery.

Ripamonti et al.[8] reported the administration of oral Zinc sulfate during radiotherapy and 1 month after complete radiotherapy in 18 head and neck cancer patients. The study revealed that the patient receiving Zinc sulfate had more rapid recovery of taste acuity than placebo arm at 1 month after complete radiotherapy with statistically significant for salty, sweet and sour tastes recognition.

Yamashita et al.[9] measured taste ability in 118 patients before radiotherapy, during radiotherapy and monthly from 4 to 14-24 months after radiotherapy between whole tongue versus partial tongue irradiation. There was a significant impairment of the threshold of all four basic tastes (sweet, sour, bitter and salt) at 3 weeks after RT and remained at 8 weeks in whole tongue irradiation patients.

In this study, it was found that Zinc amino acid chelate did not appear to decrease the incidence of taste alterations after complete radiation for head and neck cancer within 1-6 months with the sweet tastes (p=0.43), salty tastes (p=0.68) and

sour tastes (p=0.51). The relatively small number of subjects in this study may contribute to the lack of statistical differences between groups.

Conclusion

All of the taste evaluations revealed no statistical significance between the patients received with Zinc amino acid chelate and without Zinc administration (p >0.05). The relatively small number of subjects in this study may contribute to the lack of statistical differences between groups.

Acknowledgement

This study was granted by Faculty of Medicine, Khon Kaen University, Thailand (Grant Number HE531446). We would like to express our deep appreciation to Dr. Asawadech Sanbua for his vulnerable advices and to Ms. Kaewjai Thepsutamrat for statistical analysis. We would like to thank appreciation acknowledgement gives to Qualimed Company Limited for Zinc amino chelate.

References

1. Jham BC, Freire ARS. Oral complications radiotherapy in the head and neck. Braziallian of Journal otorhinolarymgology 2006;72(5):704-8.
2. Vissink A, Jansma J, Spijkervet FKL,et al. Oral sequelae of head and radiotherapy. Critical Reviews in Oral Biology and Medicine 2003;14(3):199-12.
3. Conger AD. Loss and recovery of taste acuity in patients irradiated to the oral cavity. Radiat Res 1973;53:338-47.
4. Vissink A, Burlage FR, Spijkevert FKL, et al. Prevention and treatment of the consequences of head and neck radiotherapy.Critical Reviews in Oral Biology and Medicine 2003;14(3):213-25.
5. Buntzel J, Glazel M, Kuttner K, et al. Amifostine in simultaneous radiochemotherapy of advanced head and neck cancer. Semin Radiat Oncol 2002;12:4-13.
6. Redda MGR, Allis S. Radiotherapy-induced taste impairment. Cancer treatment reviews 2006;32:541-7.
7. Halyard MY, Jatoi A, Sloan JA, et al. Does zinc sulfate prevent therapy-induce taste alterations in head and neck cancer patients? Results of phase III double blind, placebo-controlledled trial from the north central cancer treatment group. Int J Radiat Oncol Bio Phys (N01C4) 2007;67(5):1318-22.
8. Ripamonti C, Zecco E, Brunelli C, et al. A Randomized, Controlled Clinical Trial to Evaluate the Effects of Zinc Sulfate on Cancer Patients with Taste Alterations Caused by Head and Neck Irradiation. Cancer 1998;82(10): 1938-45.
9. Yamashita H, Nakagawa K, Nakamura N, et al. Relation between acute and late irradiation impairment of four basic tastes and irradiated tongue volume tongue volume in paitents with head - and - neck cancer. International Journal radiation oncology Biology and physiology 2006;66(5):1422-9.
10. Sandow PL, Yazdi MH, Heft MW. Taste loss and Recovery Following Radiation Therapy. Journal of dental research 2006;85(7):608-11.
11. Yamashita H, Nakagawa K, Tago M, et al. Taste dysfunction in patients receiving radiotherapy. Head and neck 2006;28:508-16.
12. Mattes RD. Effects of linoleic acid on sweet, sour, salty, and bitter taste thresholds and intensity ratings of adults. Am J Physiol Gastrointest Liver Physiol 2007;292:1243-8.
13. Shi HB, Masuda M, Umezaki T, et al. Irradiation impairment of umami taste in patients with head and neck cancer. Auris Nasus Larynx 2004;292:1243-8.
14. Maes A, Huygh I, Weltens C, et al. De Gustibus: time scale of loss and recovery of tastes caused by radiotherapy. Radiotherapy and oncology 2002;63:195-201.
15. Mossman KL, Henkin RI. Radiation-induced changes in taste acuity in cancer patients. Int J Radiat Oncol Biol Phys 1978;4:663-70.
16. Mossman KL. Quantitative radiation dose-response relationships for normal tissues in man. I. Gustatory tissue response during photon and neutron radiotherapy. Radiat Res 1982;91:265-74.

THE ASEAN JOURNAL OF RADIOLOGY 2012: 18(2): 85-91 85

Original Article

Determination of Parameter in The Equivalent Square Field Formulas for Estimating Head Scatter Factor of Rectangular Field

Lukkana Apipunyasopon[1], Somyot Srisatit[1], Nakorn Phaisangittisakul[2,3]

[1] *Department of Nuclear Engineering, Faculty of Engineering, Chulalongkorn University, Bangkok 10330, Thailand*

[2] *Department of Physics, Faculty of Science, Chulalongkorn University, Bangkok 10330, Thailand*

[3] *ThEP Center, CHE, 328 Si-Ayuttaya Road, Bangkok 10400, Thailand*

Abstract

An equivalent square field for estimating head scatter factor for a given rectangular field was calculable using the empirical formula introduced by Vadash and Bjarngard (Med. Phys. 20, 773-774 (1993)) and, also, the derived formula proposed by Kim et al (Med. Phys. 24, 1770-1774 (1997)). Both formulas account for the effect of field elongation and collimator exchange. In each formula, there exists only one parameter which is optimally chosen for the empirical formula and is calculated using the location of collimators for the derived formula. In this study, the head scatter factors were generated by the Eclipse AAA treatment planning system for various square and rectangular fields for 6 MV photon beam of a Varian Clinac 23EX at the depths of 0.5, 5 and 10 cm. The head scatter factors for equivalent square field obtained from both relationships were investigated. In the empirical formalism, the maximum deviation from the square field data was about 0.008 or less than 1%. The geometrical parameter was found to be consistent with the empirical parameter at the 0.5-cm depth while an obvious dissimilarity was observed at the 5-cm and 10-cm depth. Despite the difference on the parameters, however, the discrepancy between the estimated and the expected head scatter factor is considered clinically negligible in both equivalent square field formalisms.

Keywords: head scatter factor / equivalent square field / empirical formalism

Introduction

For megavoltage photon beam used in radiation oncology, a change of scattered radiation with a collimator setting that reaches the point of measurement on the central axis is described by the head scatter factor (or collimator scatter factor), which is expressed as

$$H(X_D,Y_D) = D(X_D,Y_D) / D(X_{D=10\ cm},Y_{D=10\ cm}) \quad \text{..... (1)}$$

where $D(X_D,Y_D)$ is the dose in air on the central axis at the detector plane and X_D, Y_D are the field sizes, also at the detector plane, determined by the lower (X) and upper (Y) collimator jaws, respectively. The collimator setting for reference field size is 10 x 10 cm^2. The variation of head scatter factor is usually not large. In our study, the value ranges from about 0.94 to about 1.08. In addition, the effect of collimator exchange for two different rectangular fields, i.e. the difference between $H(X_D,Y_D)$ vs. $H(Y_D,X_D)$ where $X_D \neq Y_D$, is also small (2%-3% for open fields and 3%-4% for wedged fields)[1].

Typically, the beam data from the medical linear accelerator was generally collected for various square field sizes. It is impractical to do the measurement for rectangular field since there are too many possibilities of the field size. Specifically for the determination of head scatter factor, a given rectangular field is typically related to the square field by the well-established equivalent square relationships; in the form of tables[2,3], the area-to-perimeter formula[4], and the geometric formula[5]. Generally speaking, using the formula to find an equivalent square field is more favorable than using the table due to its simplicity and convenience.

The area-to-perimeter formula[4] gives the equivalent square collimator setting for rectangular field (X_D,Y_D) according to:

$$L_{AP} = 2\ X_D\ Y_D\ /\ (X_D+Y_D). \quad \text{..... (2)}$$

This formula includes the effect of field size elongation. However, the collimator-exchange effect is not taken into account since the interchange between X_D and Y_D yields the same equivalent side L_{AP}. It also does not includes the effect from the beam's energy, the configuration of each treatment unit, and the calculated depth.

In 1993, Vadash and Bjarngard[6] proposed an empirical formula in an attempt to account for the collimator-exchange effect on the head scatter factor. The equivalent square collimator setting is given by:

$$L_{EC} = (A+1)\ X_D\ Y_D\ /\ (A\ X_D+Y_D), \quad \text{..... (3)}$$

where A is a parameter specific for each beam. This parameter is determined by minimizing the average difference between the calculated and measured head scatter factors of rectangular field. The formula is deduced to that of area-to-perimeter when A=1. The beam's energy, the configuration of treatment unit as well as the calculated depth are included in this empirical formula since the parameter is determined using the specific beam data. As the result, determination of suitable parameter needs a reliable data set of rectangular field.

Similarly, Kim et al.[7] derived a formula using the field mapping method for the calculation of an equivalent square field that gives the same head scatter factor as a given rectangular field. The derived formula has the same format as the empirical formula Eq. (3). The parameter 'A' is replaced by the geometric parameter 'k' which is obtained from the distances between the target and the top of each collimator jaw and between the bottom of each collimator jaw and the detector plane. There-

fore, this formula includes the effect from collimator-exchange, the configuration of a linear accelerator treatment head, and, also, the depth. However, the beam's energy is not accounted for in this formalism.

The purpose of this study is to determine the parameter in the empirical and the derived equivalent square field formula for calculating the head scatter factor at the depths of 0.5, 5.0 and 10.0 cm. The geometrical parameter is almost the same as the empirical parameter at shallow depths. However, they are quite different at 5 and 10-cm depth. Nevertheless, both equivalent square field formulas give the head scatter factor at three depths for rectangular field with good accuracy with the interpolated data of the square field.

Meterial and Methods

The Eclipse AAA treatment planning system was used to compute the head scatter factor for 6 MV photon beam of a Varian Clinac 23EX medical linear accelerator. A cylindrical mini-phantom with 4 cm in diameter and 20 cm in length was created in the system. The calculated points were located in the mini-phantom on its central axis at the depths of 0.5, 5 and 10 cm from the front surface using a constant source-to-surface distance of 100 cm with 100 beam monitor unit.

Due to the lack of mini-phantom in our institute, an actual measurement for the head scatter factor was unable to be performed. Nevertheless, the computed head scatter factors are reliable since the basic commissioned data had been provided to the planning system and several dosimetric quantities for both square and rectangular fields have also been validated with the measurement, for example, percentage depth dose, dose profile, beam output etc.

The first set of data was taken with the square fields ranging from 4 x 4 to 30 x 30 cm^2. The second set of data (FIX-X) was taken with the X collimator jaws fixed while the Y jaws were varied. The data with the Y collimator jaws fixed (FIX-Y) while the X jaws were varied was the third set of our data. The varied collimator settings were 4, 6, 8, 10, 12, 15, 18, 20, 22, 25, 28 and 30 cm. As a result, the opening field size ranges from 30 x 4 to 30 x 30 cm^2 for the second data set and from 4 x 30 to 30 x 30 cm^2 for the third data set.

The equivalent square field for each rectangular field was computed using the area-to-perimeter relationship (eqn. (2)), the empirical formula with varying parameter A from 0.6 to 3.0 (eqn. (3)), and the derived formula (eqn. (3) with $A=k$). The geometric parameter k's for the depths of 0.5, 5 and 10 cm are 1.52, 1.50 and 1.48, respectively. For each equivalent square field, the head scatter factor was calculated using the interpolation of the square field data. A comparison between the head scatter factor for equivalent square and for the FIX-X and FIX-Y field was then made as a function of A. The best empirical parameter A was chosen according to the minimum of the average difference as well as the maximum absolute difference.

Results

Three data sets of the head scatter factor at the 0.5, 5, and 10-cm depth are illustrated in Figure 1, where each rectangular field was converted into the equivalent square field based on the area-to-perimeter relationship, Eq. (2). The collimator-exchange effect is clearly noticed in the Figures. Additionally, the more the elongated field is, the bigger the difference is found. For the most elongated field 4 x 30 or 30 x 4 cm^2, the difference in the head

scatter factor is approximately 2% at all depths.

The head scatter factor of the equivalent square field for the FIX-X and FIX-Y data set of rectangular field was computed using the empirical formula, eqn. (3). For each value of parameter *A* ranged from 0.6 to 3.0, the difference with that of the square field was calculated. An average and the maximum of the magnitude of the difference were then evaluated for both data sets of rectangular field. These differences as a function of *A* are illustrated in Fig. 2, 3 and 4 for the depths of 0.5, 5 and 10 cm, respectively.

The minimum average difference on the head scatter factor using the empirical formula was found for *A* about 1.5, 2.0, 2.1 and for the data at 0.5, 5 and 10-cm depth, respectively. At all depths the maximum difference on the head scatter factor is less than 0.005 or approximately 0.5%. Figure 5, 6

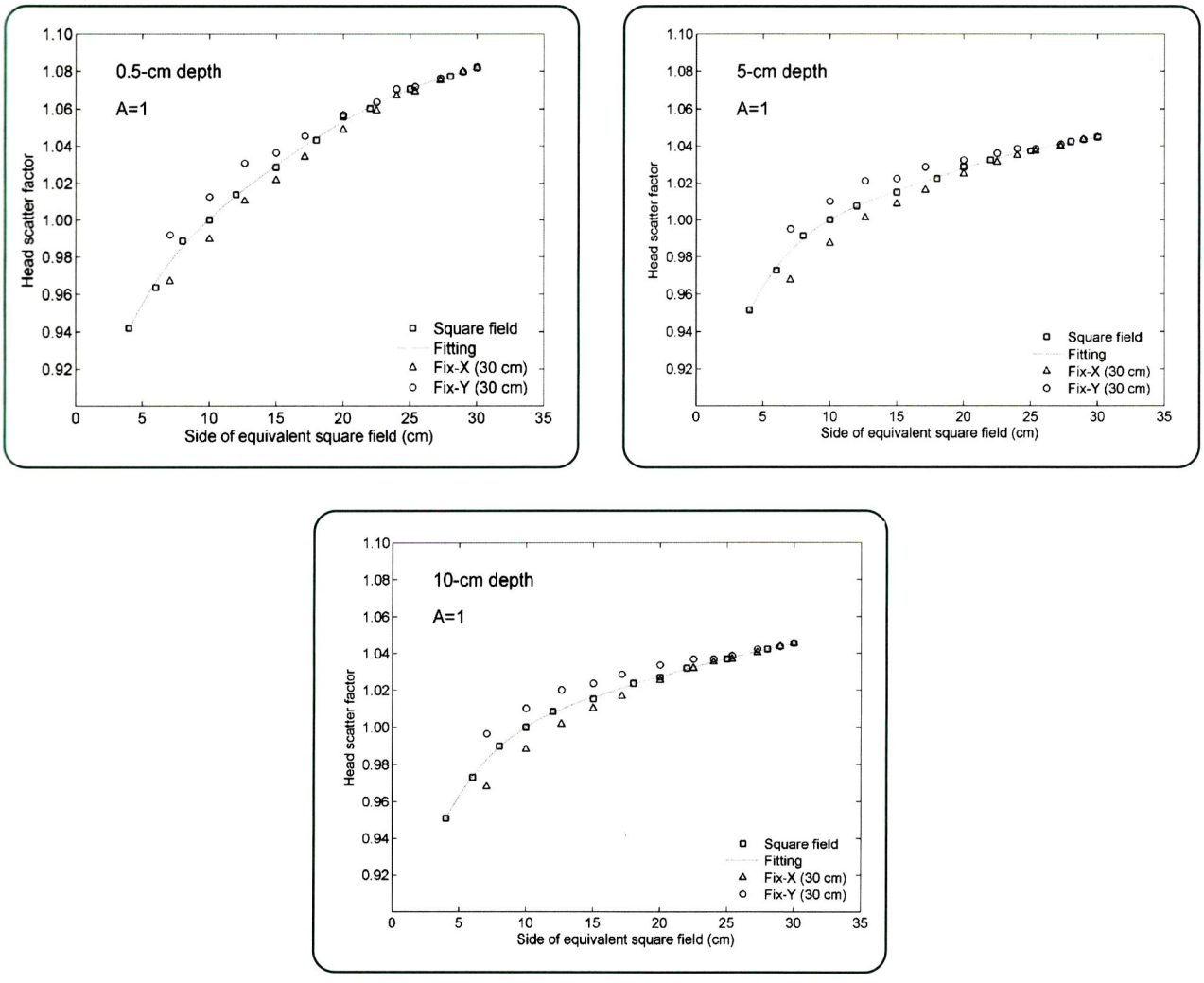

Fig.1 The head scatter as a function of square open size obtained from the area-to-perimeter method at the depth of 0.5, 5 and 10 cm for 6 MV photon beam from Varian Clinac 23EX.

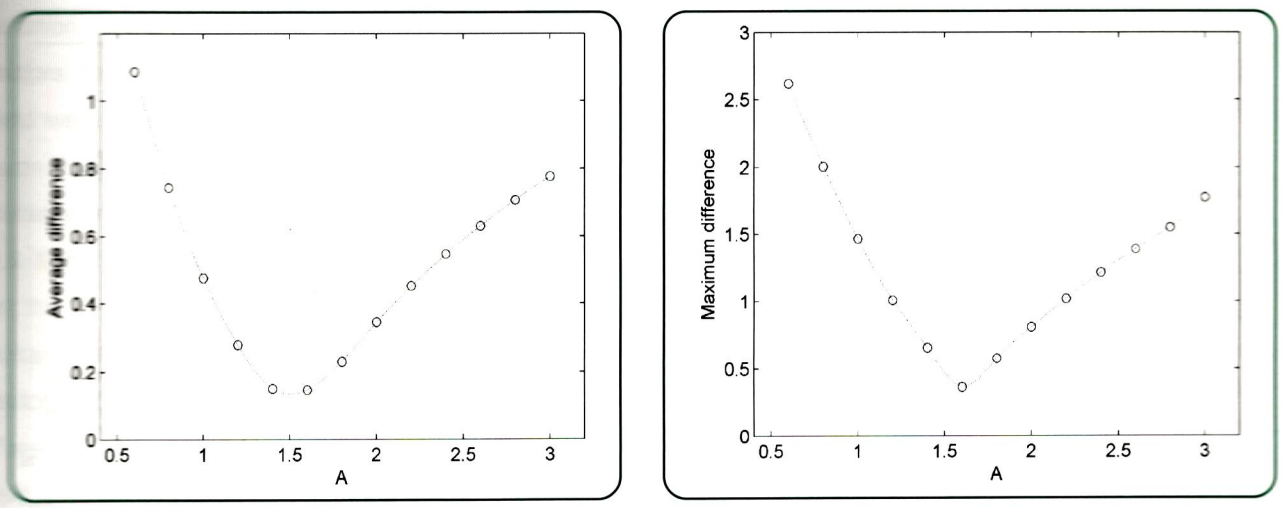

Fig.2 An average and maximun of the magnitude of difference on the head scatter factor using the empirical formula for the data at the 0.5-cm depth. The difference is scaled up by a factor of 100.

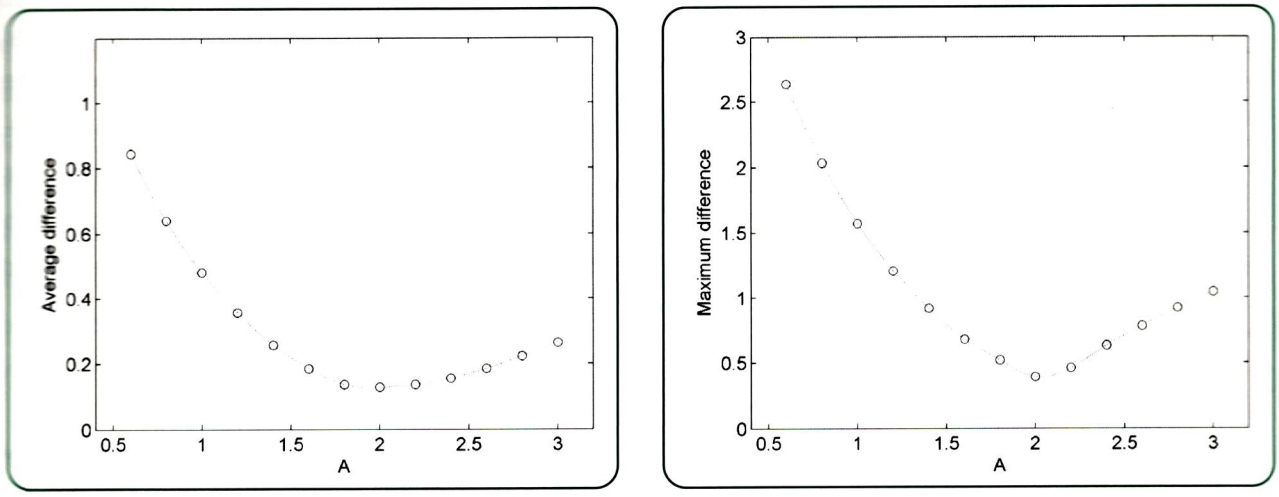

Fig.3 The same to that of Fig. 2 at the 5-cm depth.

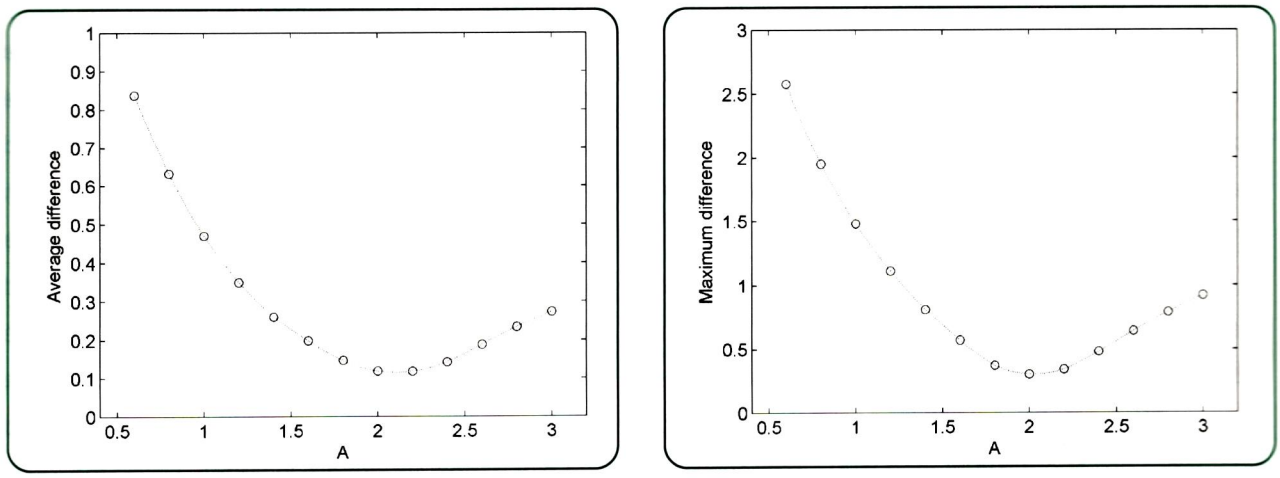

Fig.4 The same to that of Fig. 2 at the 10-cm depth.

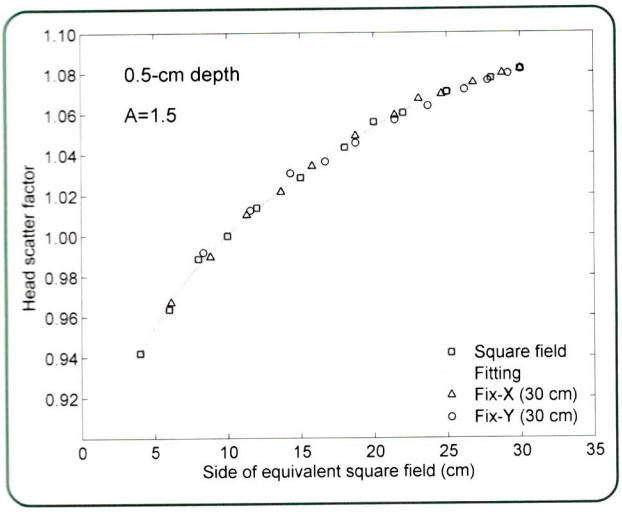

Fig.5 The coherence of head scatter factor between the equivalent square field and the square field using the best empirical parmeter at the 0.5-cm depth.

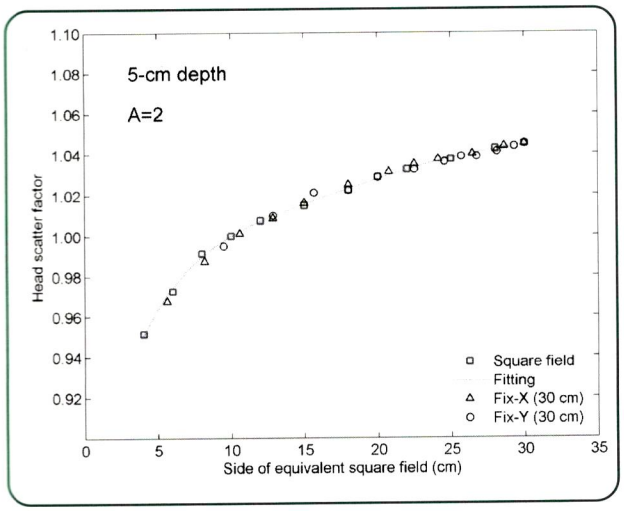

Fig.6 The same to that of Fig. 5 at the 5-cm depth.

and 7 demonstrate the coherence of head scatter factor between the equivalent square field and the square field using the best empirical parameter *A* for the depths of 0.5, 5 and 10 cm, respectively.

Using the geometric parameter k =1.48 for the head scatter factor at 10-cm depth, the difference with the square field data can be conveniently identified in Figure 4. The average and the maximum differences are about 0.0025 and 0.007, respectively.

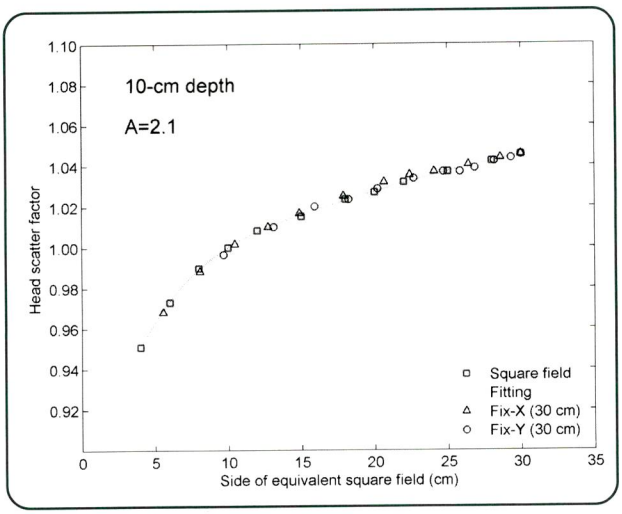

Fig.7 The same to that of Fig. 5 at the 10-cm depth.

In similar, at 0.5-cm depth where k is equal 1.52 the difference can be estimated in Figure 2. Interestingly, the empirical parameter is almost the same as the geometric parameter at the depth of 0.5-cm. In contrast, the two parameters are significantly different at 5-cm depth (2.0 versus 1.50) and 10-cm depth (2.1 versus 1.48). Nevertheless, the difference in head scatter factor is still less than 1%.

Conclusions

The head scatter factors were generated by the Eclipse AAA treatment planning system for the square fields ranging from 4 x 4 to 30 x 30 cm^2 and also for the rectangular fields with fixed-X and fixed-Y collimator setting for the field side of 30 cm while the varying side ranged from 4 to 30 cm. The equivalent square field for each rectangular field was calculated using (1) the empirical formula with different values of the parameter *A* and (2) the derived relationship with the parameter determined by the collimator settings in the linac head and the plane of interested point *k*. Both formulas have exactly the same format where both exchange and field elongation effects are included. Using the inter-

polation of the square field data, the head scatter factors for each equivalent square of rectangular field were obtained. They were then compared with each other. At depth of 0.5 cm, the optimal empirical parameter *A* that gave smallest deviation is about 1.5. It is 2.0 for the data at the 5-cm depth and 2.1 for the 10-cm depth. The derived parameter *k*'s were obtained as 1.52, 1.50, and 1.48 for the head scatter factor at the depths of 0.5, 5, and 10 cm, respectively. These two simple relationships of equivalent square field gave an acceptable estimate of the head scatter factor for rectangular field. In general, the coherence between the head scatter factors of the square field and that of the equivalent square field was found to be slightly better for the empirical formula than the derived one. However, the maximum discrepancy found in the derived relationship was still less than 1%. Since only the setting of collimators are required for calculating the geometrical parameter, the derived formula is more convenient in a practical usage. In contrast, the data base of various fields is necessary for determining parameter in the empirical formula.

References

1. Kim S, Zhu TC, Palta JR. An equivalent square field formula for determining head scatter factors of rectangular fields. Med Phys 1997;24(11):1770-4.
2. Day MJ, Aird EGA. The equivalent field method for dose determination in rectangular fields. Br J Radiol 1983; 17:105.
3. Vanselaar JLM, Heukelom S, Jager HN, Mijnheer BJ, Gasteren JJM, Kleffens HJ, et al. Is there a need for a revised table of equivalent square fields for the determination of phantom scatter correction factors? Phys Med Biol 1997;42:2369-81.
4. Sterling TD, Perry H, Katz L. Automation of radiation treatment planning. IV. Derivation of a mathematical expression for the per cent depth dose surface of cobalt-60 beams and visualization of multiple field dose distributions. Br J Radiol 1964;37:544-50.
5. Bjarngard BE, Siddon RL. A note on equivalent circles, squares, and rectangles. Med Phys 1982;9(2):258-60.
6. Vadash P, Bjarngard B. An equivalent-square formula for head scatter factors. Med Phys 1993;20(3):733-4.
7. Kim S, Zhu TC, Palta JR. An equivalent square field formula for determining head scatter factors of rectangular fields. Med Phys 1997;24(11):1770-4.

THE ASEAN JOURNAL OF RADIOLOGY 2012: 18(2): 92-100

Original Article

Location of the Mandibular Foramen from Cone Beam Computed Tomography in The Patients with Normal Occlusion

Khumpee Songkampol[1*], Natthamet Wongsirichat[2*], Raweewan Arayasantiparb[3]

[1] *Department of Oral & Maxillofacial Radiology, Faculty of Dentistry Mahidol University*

[2] *Department of Oral & Maxillofacial Surgery, Faculty of Dentistry Mahidol University*

[3] *Department of Oral & Maxillofacial Radiology, Faculty of Dentistry Mahidol University*

Abstract

Objectives: This study was to determine the location of the mandibular foramen (MF) by dental cone beam computed tomography (CBCT).

Methods: The mandibular foramen opening width (MFW) and reference lines from MF were measured in 72 patients with the normal occlusion and statistically analyzed by t-test.

Results: Comparing the left and the right side of the MFW in males was significantly different, but the other reference lines were not significantly different. In females, both the MFW and all reference lines were also not significantly different ($p > 0.05$). Comparing between sexes, the MFW was not significantly different on both side. While the reference lines of the left and right side were significantly different, the distance of the right side of the MF-IB was not significantly different ($p > 0.05$).

Conclusion: The location of the mandibular foramen was slightly posterior to the middle third of the width of the ramus and the superior to the middle third of the ramus height. This study may be useful for supplying to block the inferior alveolar nerve and in orthognathic surgery regarding bilateral sagittal split ramus osteotomy and intraoral vertical ramus osteotomy.

Keywords: cone-beam computed tomography; mandibular foramen width; mandibular foramen location; ramus of mandible; ramus osteotomy; inferior alveolar nerve block; mandibular notch

* *Corresponding author : Khumpee Songkampol, Natthamet Wongsirichat*

Introduction

The mandibular foramen is one of the foramen of the oral and maxillofacial regions, located on the inner side of the ramus. It is important in dental procedures, such as determining the length of the needle when injecting into the soft tissue in the inferior alveolar nerve block or in orthognathic surgery[1-2] including bilateral sagittal split ramus osteotomy and intraoral vertical ramus osteotomy[3].

Many previous studies of the MF in dry skulls with or without radiographs including the studies of Kositbowornchai et al.[4], Jansisyanont et al.[5], Trost et al.[6], Hwang et al.[7], and Captier et al.[8], and Haywaed et al.[9] which analyzed patients by panoramic radiographs.

The location of the MF varies, but no significant difference was observed between the left and right sides in the same sex.

Kaffe et al.[10] studied the location of the MF by using two panoramic radiographs. Afsar et al.[11] analyzed the mandibular foramen by using two views of radiographs, a panoramic and 45° oblique cephalometric radiograph.

In 2004, Tsai[12] reported locating the MF in panoramic radiographs of 311 early permanent dentition children.

Using panoramic radiographs, Trost et al.[6] studied the safety location of the mandibular foramen in intraoral vertical ramus osteotomy in vertical and horizontal planes of 46 patients.

Boonpiruk[13] studied the location of the MF related to the internal oblique ridge in the Thai dry skull. No studies of normal occlusion have been conducted among Thai patients using cone beam computed tomography (CBCT).

In addition, many locations at the inner side of the ramus are related importantly to the MF, such as the anterior border and mandibular notch, including the inferior border and posterior border of the ramus.

The aim of this study was to locate the MF and related reference lines from CBCT in Thais with normal occlusion.

Materials and methods

Seventy-two Thai patients (36 males and 36 females) aged between 20 and 40 (average age 22 years) with normal occlusion[14] and who had lower third molar surgical removal were enrolled in the study. The study used a 3D Accuitomo FPD XYZ Slice View Tomograph, model MCT-1, type EX F, J. Morita, Kyoto, Japan.

This study was approved and accepted as a clinical study by the Mahidol University Institutional Review Board with Protocol COA. No. MU-IRB 2010/264. 2109. The patients voluntarily participated in the study after informed consent. Written consent was also obtained from the patients for the study findings, and consent forms were signed in the presence of a witness for all examinations and treatment performed.

Because the field of view (FOV) of this machine is 6x6 centimeters, each patient had to undergo CBCT on left and right sides at the ramus and retromolar area. Each CBCT of the patient was analyzed by two specialized radiologists using the software supplied with the machine (i-Dixel One Data Viewer Plus Version 1.26).

For CBCT image, 78 kVp. with 4.5 mA. was used in males and 76 kVp. with 4 mA. was used in females.

Before measurement, we used the coronal view at the center of MF, and previously considered at the midpoint of the foramen and continued to measure the sagittal slice plane from this point. The radiologists made two imaginary lines on the posterior border of the ramus and inferior border of the mandible (Figure 1) and measured the center and the MF opening width (MFW) (Figure 2). The radiologists also measured the reference line from the center point of the MF (CMF) to the anterior border of the ramus (AB) (Figure 3), as well as the reference line from the CMF to the posterior border of the ramus (PB) (Figure 3). The AB-PB line was perpendicular to the imaginary line of the posterior border of the ramus.

The reference line from the CMF to the inferior point of the mandibular notch (MN) (Figure 4) and the reference line from the CMF to the inferior border of the mandible (IB) (Figure 4) were parallel to the imaginary line of the posterior border of the ramus.

The reference line from the CMF to the AB of the ramus and to the PB of the ramus was the width of the ramus. It included the reference line from the CMF to the inferior point of the MN, and the IB of the mandible was the height at the midline area of the ramus. This reference line was parallel to the posterior imaginary line.

All the data measurements were statistically analyzed by t-test at the significance level of 95%.

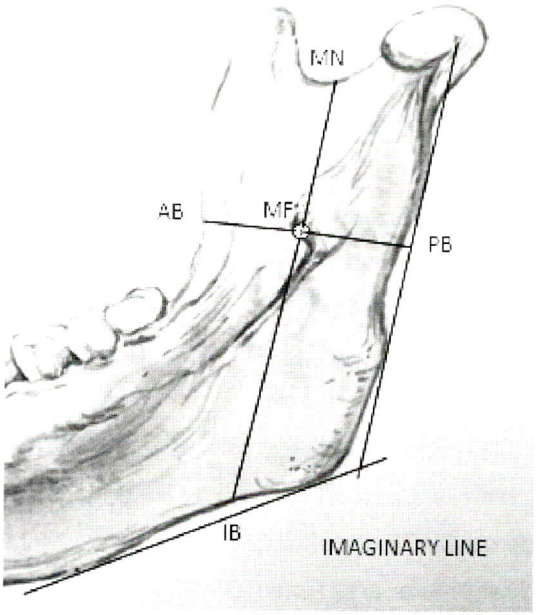

Fig.1 The imaginary line, the location of the studied mandibular foramen and reference lines studied
MF : mandibular foramina
AB : point of anterior border of the ramus
PB : point of posterior border of the ramus
MN : inferior point of the mandibular notch
IB : inferior border of the mandible

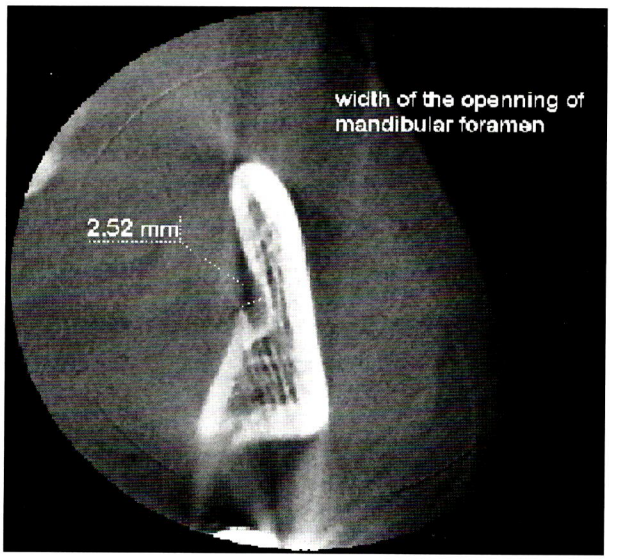

Fig.2 The center and the mandibular foramen opening width in CBCT

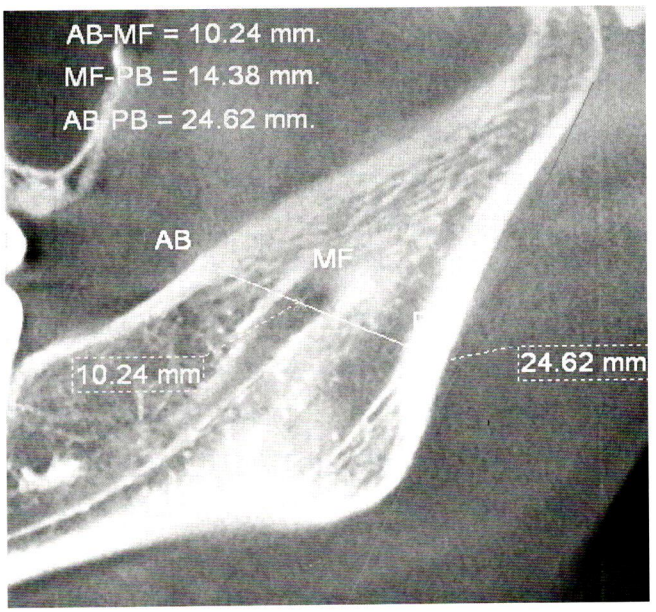

Fig.3 The reference line from the center point of the mandibular foramen to the anterior border of the ramus and the reference line from the center point of the mandibular foramen to the posterior border of the ramus

MF : mandibular foramina

AB : point of anterior border of the ramus

PB : point of posterior border of the ramus

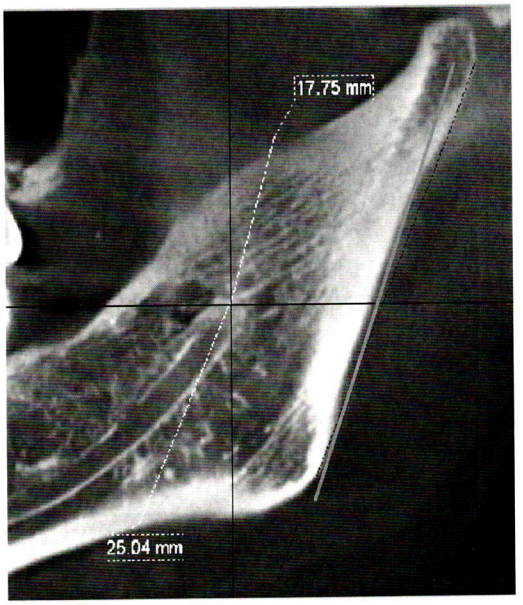

Fig.4 The reference line from the center point of the mandibular foramen to the inferior point of the mandibular notch and the reference line from the center point of the mandibular foramen to the inferior border of the mandible

Results

The range of the MFW in males was 2.01 to 4.47 mm. on the left side and 2.49 to 4.53 mm. on the right side, with the average of both sides at 3.14 mm., and in females, 2.22 to 4.17 mm. on the left side and 2.41 to 4.25 mm. on the right side with the average of both sides at 3.25 mm.

The mean reference line from the center point of the MF-AB of the ramus in males and females was 15.07 mm. and 14.40 mm, respectively. Also, the mean reference line from the CMF to the inferior point of the MN in males and females was 20.76 mm. and 19.68 mm, respectively.

Table 1 shows the mean MFW and the reference lines, with significant differences in the MFW in males of the left and right sides, but without significant difference in females. No significant differences were observed in the reference lines of the left and right sides in females and males ($p > 0.05$).

No significant differences were found ($p > 0.05$) in all reference lines, comparing between left and right sides for each sex.

When all reference lines were compared between the sexes of each side, most were significantly different ($p > 0.05$) except both sides of the MFW and the reference line of the MF to the inferior border of the mandible of the right side between sexes had no significant difference ($p > 0.05$).

Figures 5 also shows the distributions of the left and right sides of the MFW, ramus width from the PB-AB (Figure 6), and the ramus height from the MN-IB of the mandible in 36 males and 36 females (Figure 7).

The location of the MF was slightly posterior to the middle third of the width of the ramus and the superior to the middle third of the ramus height.

Table 1 Mean mandibular foramen widths and reference lines of the left and right sides in 36 males and 36 females

Measurement ($\bar{X}$ ±S.D.) (mm)		MFW	AB-MF	MF-PB	AB-PB	MF-MN	MF-IB
Male	Right	3.02±0.51	15.28±1.92	14.17±1.73	29.45±3.06	20.86±3.29	28.57±3.28
	Left	3.26±0.66	14.86±1.95	14.32±1.84	29.18±3.25	20.66±2.89	28.91±3.33
	p-value	0.009*	0.083	0.472	0.270	0.105	0.085
Female	Right	3.22±0.44	14.45±1.62	13.42±1.14	27.87±2.51	19.66±2.83	28.17±3.20
	Left	3.27±0.45	14.34±1.43	13.37±1.16	27.71±2.20	19.69±2.60	28.19±2.47
	p-value	0.602	0.413	0.705	0.314	0.910	0.932
Right side of male - female	p-value	0.283	0.003*	0.001*	0.0005*	0.002*	0.079
Left side of male - female	p-value	0.543	0.023*	0.0004*	0.0008*	0.009*	0.03*

* Significance level $p < 0.05$

MFW : mandibular foramen opening width
MF : mandibular foramen
AB : point of anterior border of the ramus
PB : point of posterior border of the ramus
MN : inferior point of the mandibular notch
IB : inferior border of the mandible

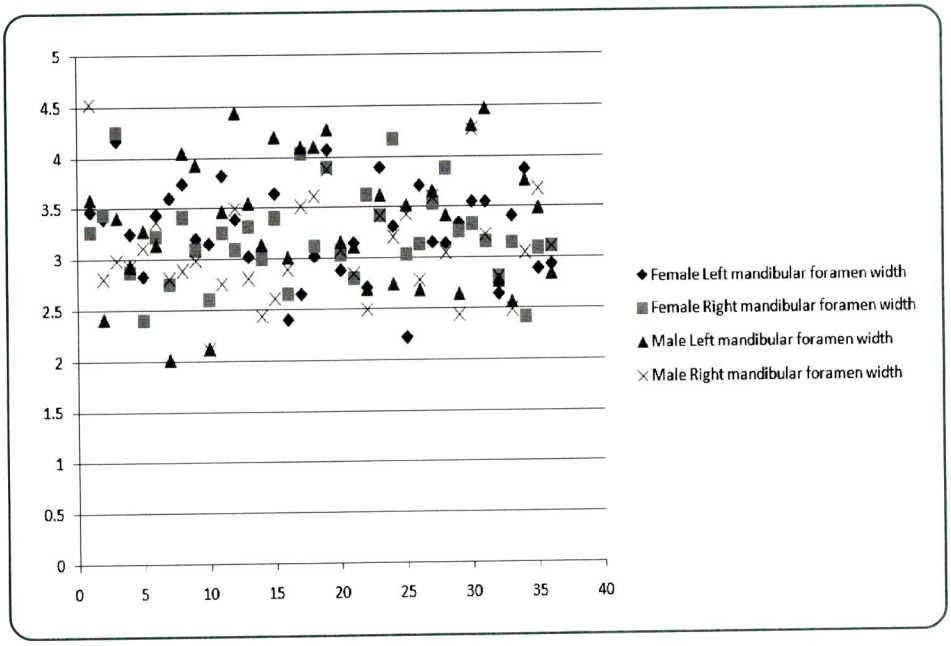

Fig.5 Distribution of the left and right mandibular foramina width in 36 males and 36 females

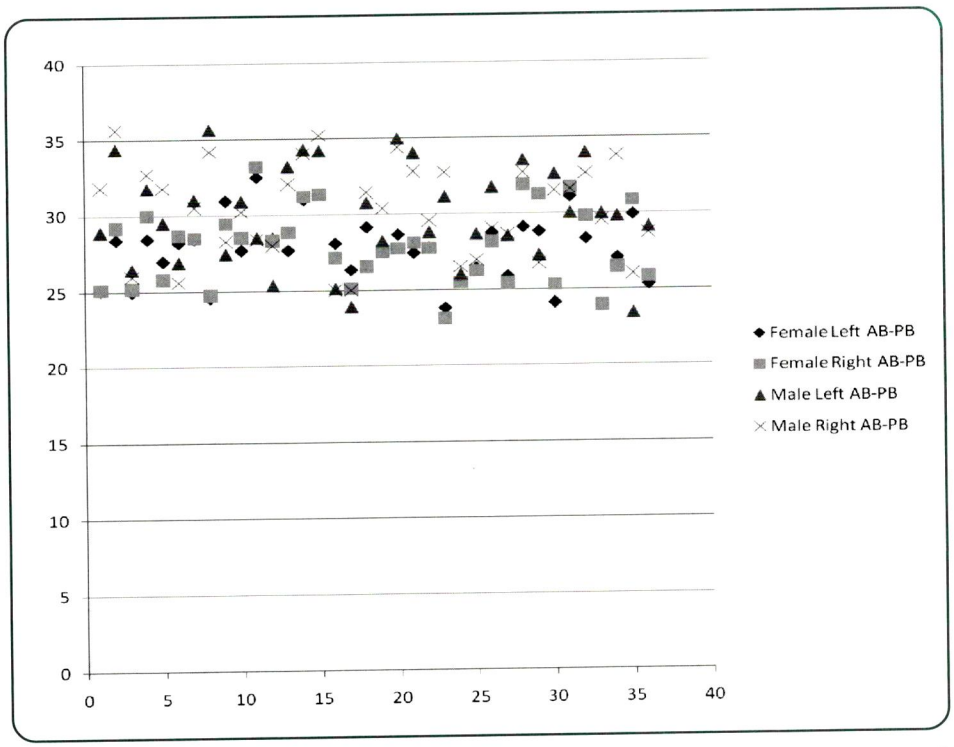

Fig.6 Distribution of the left and right of ramus width from posterior border to anterior border in 36 males and 36 females

AB : point of anterior border of the ramus

PB : point of posterior border of the ramus

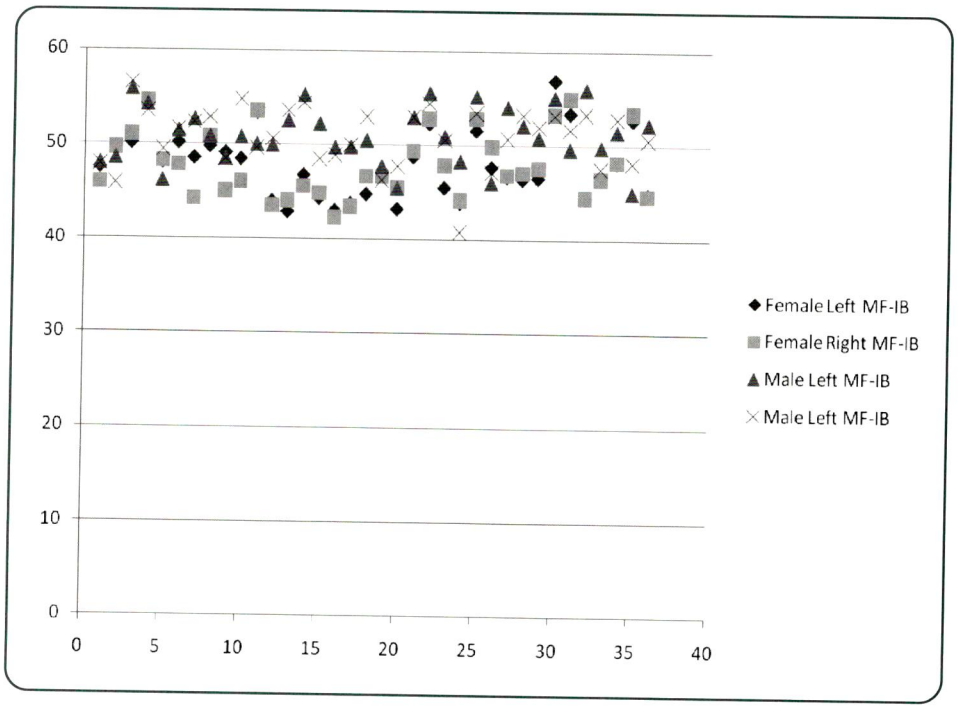

Fig.7 Distribution of the left and right side from the mandibular notch to the inferior border of the mandible in 36 males and 36 females
MF : mandibular foramina
IB : inferior border of the mandible

Discussion

Many previous studies of MF and reference lines have been conducted on dry skulls[4-9] and in patients using panoramic radiographs.[10-12,15] The study in the dry skull may lack reliable biographical data. The 3D Accuitomo FPD XYZ Slice View Tomograph is a machine that can study three dimensions of the skull[16,17] and we used CBCT 6x6 centimeters, taking right and left ramus in each patient.

As the CBCT, providing an accurate measurement,[1,18,19] we used the coronal view at the CMF, and considered at the midpoint of the foramen and measurement the MFW. Then we continued to measure the sagittal slice plane from this point, making two imaginary lines on the posterior border of the ramus and inferior border of the mandible to measure the reference line. In addition, each CBCT of the patient was adjusted, and the mean MFW and the reference lines were analyzed by two specialized oral and maxillofacial radiologists.

As for the inferior alveolar nerve block, previous studies have been conducted about the length of the needle for injection into the soft tissue[20] and the bilateral sagittal split ramus osteotomy related to the MF.[2,21]

Previous studies in Thais were conducted on dry skulls, not human beings, such as the study of, Kositbowornchai et al.[4], Jansisyanont et al.[5] and Boonpiruk.[13] We aimed to study the location of the MF and the MFW in Thais using normal occlusion by CBCT.

The previous studies of the location of the MF

in the antero-posterior plane, Kositbowornchai et al.[4] and Jansisyanont et al.[5] reported the location of the MF from dry skulls was slightly posterior. However, Hayward et al.[9] studied dry skulls, and reported the location of the MF of dry skulls in Asian and American races were not significantly different, and were located at the third quadrant from the anterior. In 2010, Trost et al.[6] found that the location of the MF was the center of the anterior two thirds and the posterior one third of the ramus. This study found the location of the MF was slightly posterior to the middle third, or near the center point of the ramus width in the antero-posterior plane.

In the supero-inferior plane, the location of the MF is mostly superior to the middle third of the ramus height from the MN to the IB of the mandible. This study is similar to the studies of Jansisyanont et al.[5], Trost et al.[6], Hwang et al.[7], and Captier et al.[8]

Hayward et al.[9] studied the MFW and reference lines comparing left and right sides, reporting no significant differences. While the MFW of the left and right sides of males was significantly different, other studies were similar to the study of Hayward et al.

This study of the reference line of the AB of the ramus to the MF in males and females indicated an average between 15.07 mm. and 14.40 mm. Needle insertion into the soft tissue should not penetrate too far into the inferior alveolar nerve block.

In addition, the reference line of the MF-MN in males and females was 20.76 mm. and 19.68 mm., respectively. It is useful in orthognathic surgery regarding bilateral sagittal split ramus osteotomy and intraoral vertical ramus osteotomy.

This study also compared the MF and reference line, between sexes showing that the MFW of both sexes and the reference line of MF-IB of the mandible were not significantly different. The other reference lines of AB-MF, MF-PB, AB-PB, MF-MN, and MF-IB were significantly different.

In conclusion, the location of the MF is slightly posterior to the middle third of the ramus width in the antero-posterior plane, and the supero-anterior plane of the MF is superior to the middle third of the ramus height from the MN-IB of the mandible. A comparison of both sides for both sexes was also not significantly different, except the MFW in the males.

Acknowledgements

First, we would like to thank the patients who participated in this study. We wish to thank the Oral & Maxillofacial Surgery and Radiology Department, Faculty of Dentistry, Mahidol University for supporting the patients. The Oral and Maxillofacial Radiology Department should also be thanked for providing and using 3D Accuitomo FPD XYZ Slice View Tomographs, J. Morita, Kyoto, Japan for this study, including SIAMDENT CO.LTD. which provided with some support for the research fund. We would like to thank the fourth year dental students, who collected related articles and data in the final preparation of the manuscript.

Declarations: None

Funding: None

Competing Interests: None declared

Ethical Approval: This study was approved and accepted as a clinical study by the Mahidol University Institutional Review Board with Protocol COA.No.MU-IRB 2010/264.2109.

References

1. Cevidanes LH, Bailey LJ, Tucker GR, Jr., Styner MA, Mol A, Phillips CL, et al. Superimposition of 3D cone-beam CT models of orthognathic surgery patients. Dento-maxillofac Radiol 2005;34(6):369-75.
2. van Merkesteyn JP, Zweers A, Corputty JE. Neurosensory disturbances one year after bilateral sagittal split mandibular ramus osteotomy performed with separators. J Craniomaxillofac Surg 2007;35(4-5):222-6.
3. da Fontoura RA, Vasconcellos HA, Campos AE. Morphologic basis for the intraoral vertical ramus osteotomy: anatomic and radiographic localization of the mandibular foramen. J Oral Maxillofac Surg 2002;60(6):660-5.
4. Kositbowornchai S , Siritapetawee M, Damrongrungruang T, Khongkankong W, Chatrchaiwiwatana S, Khamanarong K, et al. Shape of the lingula and its localization by panoramic radiograph versus dry mandibular measurement. Surg Radiol Anat 2007:29:689-94.
5. Jansisyanont P, et al. Shape, Height, and Location of the Lingula for Sagittal Ramus Osteotomy in Thais. Clin Anat 2009;22(7):787-93.
6. Trost O, Salignon V, Cheynel N, Malka G, Trouilloud P. A simple method to locate the mandibular foramen: preliminary radiological study. Surg Radiol Anat 2010; 32(10):927-31.
7. Hwang TJ, Hsu SC, Huang QF, Guo MK. Age changes in location of mandibular foramen. Zhonghua Ya Yi Xue Hui Za Zhi 1990;9(3):98-103.
8. Captier G, Lethuilier J, Oussaid M, Canovas F, Bonnel F. Neural symmetry and functional asymmetry of the mandible. Surg Radiol Anat 2006;28(4):379-86.
9. Hayward J, Richardson ER, Malhotra SK. The mandibular foramen: its anteroposterior position. Oral Surg Oral Med Oral Pathol 1977;44(6):837-43.
10. Kaffe I, Ardekian L, Gelerenter I, Taicher S. Location of the mandibular foramen in panoramic radiographs. Oral Surg Oral Med Oral Pathol 1994;78(5):662-9.
11. Afsar A, Haas DA, Rossouw PE, Wood RE. Radiographic localization of mandibular anesthesia landmark. Oral Surg Oral Med Oral Pathol 1998;86(2):234-41.
12. Tsai HH. Panoramic radiographic findings of the mandibular foramen from deciduous to early permanent dentition. J Clin Pediatr Dent 2004;28(3):215-20.
13. Boonpiruk N. Location of MF in Thai people. J Dent Assoc Thai 1975;25(4):173-7.
14. Andrews LF. The six keys to normal occlusion. AJO-DO 1972;76:296-309.
15. Laster WS, Ludlow JB, Bailey LJ, Hershey HG. Accuracy of measurements of mandibular anatomy and prediction of asymmetry in panoramic radiographic images. Dentomaxillofac Radiol 2005;34(6):343-9.
16. Hetson G, Share J, Frommer J, Kronman JH. Statistical evaluation of the position of the mandibular foramen. Oral Surg Oral Med Oral Pathol 1988;65(1):32-4.
17. Lofthag-Hansen S, Thilander-Klang A, Ekestubbe A, Helmrot E, Grondahl K. Calculating effective dose on a cone beam computed tomography device: 3D Accuitomo and 3D Accuitomo FPD. Dentomaxillofac Radiol 2008; 37(2):72-9.
18. Kobayashi K, Shimoda S, Nakagawa Y, Yamamoto A. Accuracy in measurement of distance using limited cone-beam computerized tomography. Int J Oral Maxillofac Implants 2004;19(2):228-31.
19. Loubele M, Bogaerts R, Van Dijck E, Pauwels R, Vanheusden S, Suetens P, et al. Comparison between effective radiation dose of CBCT and MSCT scanners for dentomaxillofacial applications. Eur J Radiol 2009;71(3): 461-8.
20. Srisopark SS, Hatajid P. Optimal needle penetration in inferior alveolar nerve block. J Dent Assoc Thai 1982;32 (3):83-92.
21. Nicholson ML. A study of the position of the mandibular foramen in the adult human mandible. Anat Rec 1985; 212(1):110-2.

THE ASEAN JOURNAL OF RADIOLOGY 2012: 18(2): 101-107 101

Original Article

The Effect of Zinc Amino Acid Chelate on Decrease of Taste Dysfunction in Head and Neck Cancer Patients During Radiotherapy, A Prospective Randomized Controlled Trial

Asawadech Sanbua, Montien Pesee, Srichai Krusun, Vorachai Tangvoraphonkchai, Chunsri Supaadirek, Komsan Thamronganantasakul, Prawat Padoongcharoen.

Division of Radiotherapy, Radiology Department, Faculty of Medicine, Khon Kaen University, Thailand, 40002

Abstract

Objectives: To prospectively investigate whether Zinc amino acid chelate on decrease of taste dysfunction in head and neck cancer patients treated with radiotherapy alone or concurrent chemoradiotherapy during radiotherapy.

Materials and Methods: Between September 2010 and March 2011, forty-three patients were randomized to receive either Zinc or no Zinc administration, 20 patients received Zinc amino acid chelate and 23 patients without amino acid chelate administration. The taste evaluation at 1st week was found to be better in sweet, salty and sour taste than the weeks after. The taste dysfunction was found to be decrease when receiving radiation doses of 20Gy/2weeks and it continued taste dysfunction through complete radiotherapy. The study demonstrated no statistically significant on baseline taste function, taste dysfunction during radiotherapy of doses 20-50Gy/2-5weeks of the both groups (p >0.05).

Conclusions: All of the taste evaluations revealed no statistical significance between the patients received with Zinc amino acid chelate and without Zinc administration (p >0.05). The relatively small number of subjects in this study may contribute to the lack of statistical differences between the both groups.

Keywords: Zinc amino acid chelate, radiotherapy, taste dysfunction

Introduction

Head and neck cancer is one of the most prevalence cancer[1]. In advanced stages, treatments should be multimodality such as combined surgery with adjuvant radiotherapy and/or chemotherapy. The common acute complications of radiation therapy are taste dysfunction, oral mucositis and dry desquamation[2]. The condition of taste dysfunction had been detected for several reasons, such as direct damage in taste buds and salivary glands, toxic substances, radiation, chemotherapy[3] and drugs[4,5]. The major cause of radiation effect on taste dysfunction was the disappearance of irradiated taste buds[6-11]. This morbidity was found in the 1st week of radiotherapy, increased more in the 2nd weeks (about 20 Gy/2weeks) and most common when the taste buds were irradiated to 40-60 Gy /4-6 weeks[11]. This condition could be return to normal function after definitive radiotherapy within 8 weeks on patients with partial tongue and 6 months of whole tongue irradiation[12]. Prevention of taste dysfunction from exposure radiotherapy by using cytoprotective agent and pushing the tongue out of the radiation fields including Zinc supplementary had been reported in good outcome[13].

Zinc is the essential mineral for repairing damaged cells after inflammation in mucositis of the mouth. Zinc also preserves taste disorders in patients with low Zinc level[14,15]. Zinc is the one substance that binds to the taste-papilla and stimulates it to taste process. In addition, Zinc supports lubricant of saliva process [16]. Moreover, Zinc elements relate to the gustatory nerve activity[17,18]. The Thai Recommended Daily Intakes 1999 suggested daily consumption of Zinc element at 15 mg/day, Zinc elements for person per day was 6.3±0.2 mg in males and 5.5±0.2 mg in females[18]. Inadequate Zinc elements from food had been reported and led to taste dysfunction[19].

The $ZnSo_4$ has competitive binding with receptor of Copper. Another form of Zinc elements such as Zinc amino acid chelate which demonstrates no competitive binding with the receptor of Copper. The reviews show none of reports of using Zinc amino acid chelate for preventing taste dysfunction among Thai cancer patients. This randomized controlled trial was therefore conducted to determine whether the effect of Zinc amino acid chelate on decrease of taste dysfunction in head and neck cancer patients treatment with radiotherapy alone or concurrent chemoradiotherapy.

Materials and Methods

This prospective randomized controlled trial was performed at Division of Radiotherapy, Department of Radiology, Faculty of Medicine, Khon Kaen University, Thailand, between September 2010 and March 2011. This project has been approved by the Human Ethics Committee of Khon Kaen University (HE 531130). Inclusion criteria were (1) head and neck cancer patients treated with radiotherapy covering the mouth. (2) age 20 to 70 years. Exclusion criteria (1) had undergone surgery of the tongue. (2) receiving drug cytoprotective agent, captopril, penicillamine and metronidazole. (3) receiving previous radiotherapy of head and neck region. (4) who had undergone surgery on organs of the smell associated with taste. (5) pregnant or during lactation. (5) history of oral contraceptives therapy. The statistical analysis was performed by using the STATA software version 10 and SPSS software version 13. A *p*- value of less than 0.05

was considered statistically significant. The results of taste evaluation were calculated by Repeated-measures ANOVA method.

The patients were randomized by using simple random sampling to receive either Zinc amino acid chelate or non- Zinc amino acid chelate administration. The patients received doctor's explanation and also signed consent for research participation as follows: - (1) Both groups of the patients were evaluated the baseline taste function before radiotherapy and week by week from the first week up to the 5th week of radiation by using taste substances and concentration followed by Yamashita H, et al[20]. (2) Patients in experimental group were received Zinc amino acid chealate 15 mg once daily with irradiation or radiochemotherapy from the first day of irradiation until the completion of radiotherapy. The patients in control group were treated with irradiation or radiochemotherapy without Zinc administration. (3) This study used sucrose to test sweet. These substances used in liquid form and tested by dropping on the papilla from lowest to highest concentration and recorded minimum concentration that patients can distinguish the taste, sodium chloride was used for salty taste and tartaric acid was used for sour taste. (4) Participants will gargle before the next time of taste evaluation. The measure used score 0-4 compared to Subjective Total Taste Acuity (STTA) scale[10]. (5) Test all patients irradiated at 20Gy, 30Gy, 40Gy and 50Gy. The score were recorded form of visual analog scale. (6) In order to measure taste function, the patients rated score by themselves and viewed the past score.

Results

Patient characteristics are summarized in Table 1, the diagnosis of disease in Table 2, the radiation techniques in Table 3, and the concentration of taste substances in Table 4.

The analysis of taste function found that the sweet, salty and sour tastes revealed no statistical significance between the patients received with Zinc amino acid chelate and without Zinc amino acid chelate administration (p=0.95, p=0.32 and p=0.62). The taste evaluation in the first week was better than the second through the fifth irradiated week with statistical significance (p <0.001) as shown in Figure 1-2.

The multivariate analysis of concurrent chemo-radiation or radiation alone and with or without Zinc amino acid chelate administration found that no

Table 1 Patient Characteristics

	Characteristic	Zinc (N=20)	No zinc (N=23)	*p*-value
Sex	Male	13	13	0.57
	Female	7	10	
Age	≤60 years old	13	20	0.09
	>60 years old	7	3	
Smoke	Yes	9	7	0.32
	No	11	16	
Drink	Yes	6	3	0.74
	No	14	15	

Table 2 The diagnosis of patients

Diagnosis	Zinc (N=20)	No zinc (N=23)	*p*-value
Oropharyngeal carcinoma	1	5	
Base of tongue carcinoma	1	2	
Parotid gland carcinoma	0	2	
Nasopharyngeal carcinoma	8	6	0.54
Oral tongue carcinoma	2	2	
Maxilla and nasal cavity carcinoma	1	1	
Oral cavity carcinoma	4	1	
Hypopharyngeal carcinoma	3	2	
Diffuse large B cell lymphoma	0	1	

Table 3 Modalities of therapy and radiation techniques

		Zinc (N=20)	No zinc (N=23)	*p*-value
Volume of tongue	Partial tongue irradiation	11	15	0.49
	Whole tongue irradiation	9	8	
Technique	2D conventional irradiation	19	23	0.27
	3D conformal irradiation	1	0	
CCRT	Yes	14	16	0.96
	No	6	7	

Table 4 Baseline taste evaluations before radiotherapy

	Concentrate	Zinc (N=20)	No zinc (N=23)	*p*-value
Sucrose	8.8 mM	5	3	0.48
	73 mM	8	13	
	0.29 M	7	7	
Sodium chloride	52 mM	7	15	0.21
	0.22 M	10	7	
	0.86 M	2	1	
	1.7 M	1	0	
Tartaric acid	1.3 mM	5	4	0.61
	13 mM	11	16	
	0.13 M	4	3	

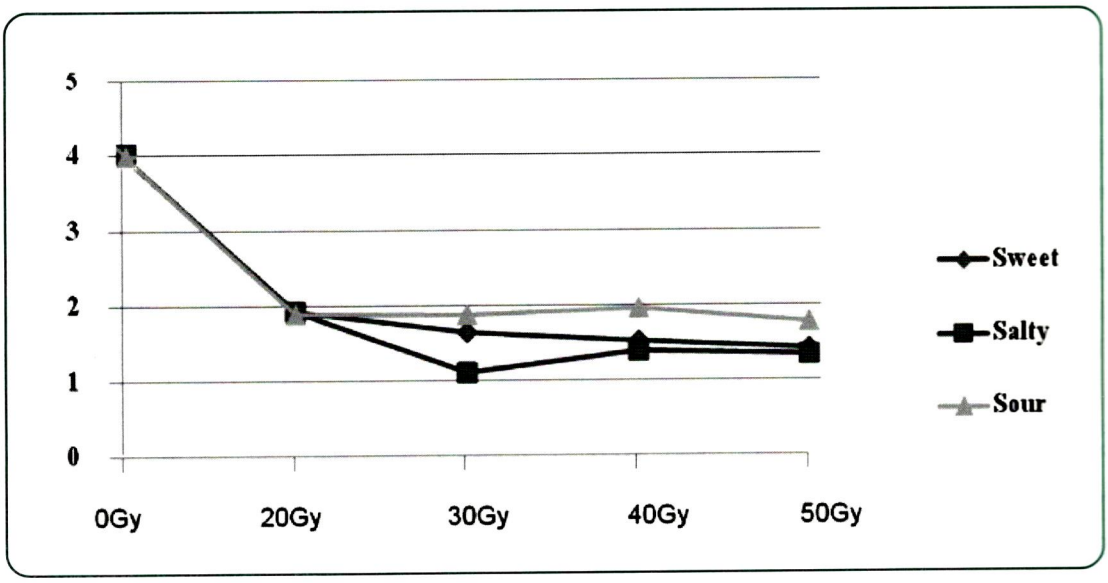

Fig.1 The difference of tastes evaluation

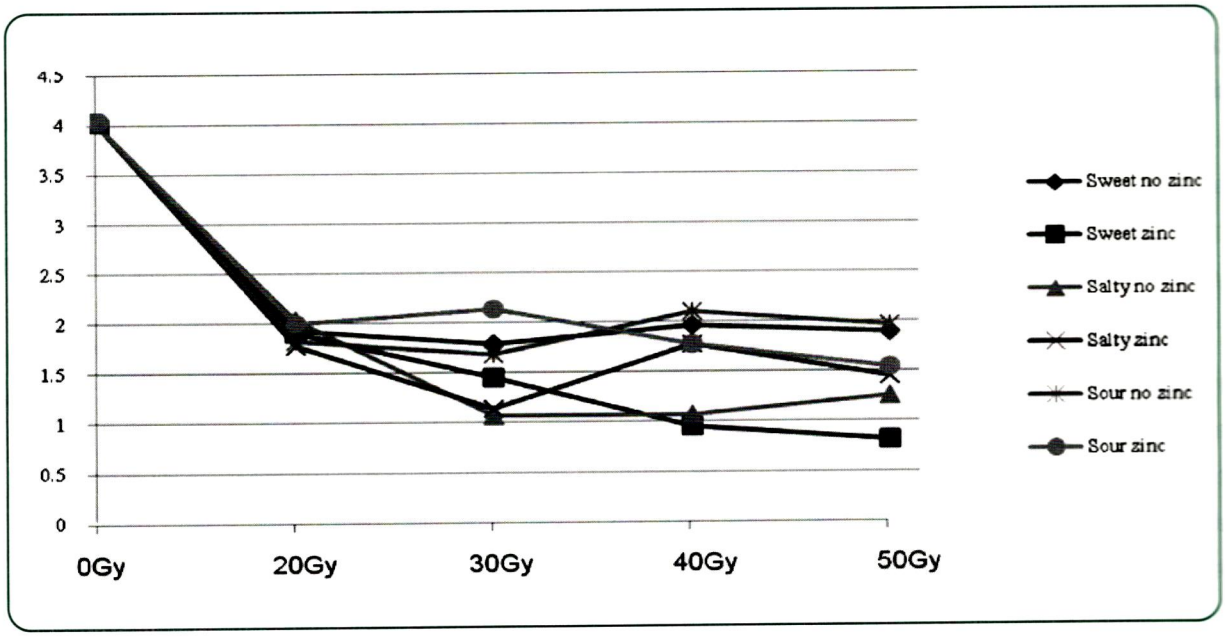

Fig.2 The difference of taste evaluation with or without Zinc amino acid chelate administration

statistical significance between the patients received with Zinc and without Zinc administration in all of taste (sweet ; p = 0.39, salty; p = 0.17 and sour ; p = 0.97). The analysis of partial and whole tongue irradiation with or without Zinc amino acid chelate administration found that no statistical significance in both groups (sweet; p = 0.17, salty; p = 40 and sour; p = 0.38).

Discussion

The benefit of Zinc sulfate therapy in reducing the occurrence of taste disorders during radiotherapy had been reported[16]. The improving taste function by using Zinc picolinate had been reported in patients with Zinc deficiency or idiopathic taste disorders[21]. The treatment prophylaxis before irradiation in patients with Zinc ion therapy demonstrated less severe hypogeusia than without Zinc therapy[22]. Kitago H, et al. found the benefit of Zinc therapy in improving taste function[23]. Some report demonstrated no benefit of taste alterations by using Zinc sulfate therapy during irradiation[24]. The study of Zinc gluconate revealed benefit for patients with idiopathic and Zinc-deficient taste disorder[25]. The improvement of taste perception had been reported by Zinc element administration[26].

The present study demonstrated taste dysfunction during irradiation of 20Gy/2weeks comparable to some studies 16,20,27. The sweet, salty and sour taste evaluations in the first week were better than the second through the fifth irradiated week with statistical significance (p <0.001). The sweet taste of this study revealed no statistical significance between the patients received with Zinc amino acid chelate and without Zinc (p = 0.46). The salty taste of this study revealed no statistical significance between the patients received with Zinc amino acid chelate and without Zinc (p = 0.17). The sour taste of this study revealed no statistical significance between the patients received with Zinc amino acid chelate and without Zinc (p = 0.79).

Conclusions

The present study demonstrated taste dysfunction during irradiation of 20Gy/2weeks. The sweet, salty and sour taste evaluations in the first week were better than the second through the fifth irradiated week with statistical significance (p <0.001). All of the taste evaluations revealed no statistical significance between the patients received with Zinc amino acid chelate and without Zinc amino acid chelate administration (p >0.05). The relatively small number of subjects in this study may contribute to the lack of statistical differences between groups.

Acknowledgement

This study was granted by Faculty of Medicine, Khon Kaen University, Thailand (Grant Number HE531130). The authors would like to express our deep appreciation to Prof. Dr. Arun Chirawatkul for methodology comments and Miss Jitjira Chaireat for statistical analysis. Appreciation acknowledgement gives to Qualimed Company Limited for Zinc amino chelate. There is no conflict of interest regarding this research.

References

1. Martin N, Patel N .Cancer incidence and leading site. Cancer In Thailand Vol IV (1998-2000), 2000;7-21.
2. Hansen KE, Roach M. Cancer of the Lip and Oral Cavity. In Mould, Eric K. Hansen, Sue S. Yom, Chien Peter Chen eds. Handbook of Evidence-Based Radiation Oncology 2nd Edition. London. Springer 2010;143.

3. Terrance BC, Joel BE, Christo M. Taste and smell dysfunction in patients receiving chemotherapy: A review of current knowledge. Support Care Cancer 2001;9:575-80.
4. Schiffman SS, Gatlin AC. Clinical physiology of taste and smell. Annu. Rev. Nutr 1993;13:405-36.
5. Henkin R. Decreased taste sensitivity after d-penicillamine reversed by Copper administration. The lancet 1967;290 (7529):1268-71.
6. Thiel HJ, Fietkau R, Sauer R. Malnutrition and the role of nutritional support for radiation therapy patients. Recent Results in Cancer Research 1988;108:205-26.
7. Westin T, Jansson A, Zenckert C, et al. Mental depression is associated with malnutrition in patients with head and neck cancer. Archives of Otolaryngology-Head & Neck Surgery 1988;114:1449-53.
8. Lee J. Incidence of weight loss in head and neck cancer patients on commencing radiotherapy treatment at a regional oncology centre. European Journal of Cancer Care (England) 1999;8:133-6.
9. Fang FM, Chiu HC, Kuo WR, et al. Health-related quality of life for nasopharyngeal carcinoma patients with cancer-free survival after treatment. Int J Radia Oncol Bio Phys 2002:53:959-68.
10. Vissink A, Burlage FR, Spijkervet FK, et al. Prevention and treatment of the consequences of head and neck radiotherapy. Critical Revues of Oral Biological Medicine, 2003;14:213-25.
11. Kamprad F, Ranft D, Weber A, et al . Functional Changes of the Gustatory Organ Caused by Local Radiation Exposure during Radiotherapy of the Head-and-Neck Region. Strahlenther Onkol 2008;184:157-62.
12. Büntzel J, Schuth J , Klaus K, et al . Radiochemotherapy with amifostine cytoprotection for head and neck cancer. Support Care Cancer 1998;6:155-60.
13. Lin L-C, Que J, Lin L-K, et al . Zinc supplementation to improve mucositis and dermatitis in patients after radiotherapy for head-and-neck cancers: A double-blind, randomized study. Int J Radiat Oncol Biol Phys 2006;65(3): 745-50.
14. Rosado LJ. Zinc and Copper: Proposed Fortification Levels and Recommended Zinc Compounds. The Journal of nutrition 2003;2985-9.
15. Keast R.S.J (2003). The Effect of Zinc on Human Taste Perception, Sensory and Nutritive Qualities of Food. Journal of food science 2003;68:5.
16. Ripamonti C, Zecca E, Brunelli C, et al. A randomized, controlled clinical trial to evaluate the effect of Zinc sulfate on cancer patients with taste alterations caused by head and neck irradiation. Cancer 1998;82(10):1938-45.
17. Songchitsomboon S, Komindr S, Piaseu N, et al. Zinc and Copper intake and sources in healthy adults living in Bangkok and surrounding districts. Biol Trace Elem Res. 1998;61(1):97-104.
18. Yokoi K. Association between plasma Zinc concentration and Zinc kinetic parameters in premenopausal women. Am J Physiol Endocrinol Metab 2003;285:E1010-20.
19. Bolze MS, Fosmire GJ, Stryker JA, et al. Taste Acuity, Plasma Zinc Levels and Weight loss during Radiotherapy: A Study of Relationships. Radiology 1982;163-9.
20. Yamashita H, Nakagawa K, Tago M, et al. Taste dysfunction in patients receiving radio therapy. Head Neck 2006; 28(6):508-16.
21. Sakai F, Yoshida S, Endo S, et al. Double-blind, Placebo-controlled Trial of Zinc Picolinate for Taste Disorders. Acta Otolayngol 2002;546:129-33.
22. Henkin RI, Keiser HR, Jafee IA, et al. Prevention and treatment of hypogeusia due to head and neck irradiation. JAMA 1972;220:870-1.
23. Kitago H., Tomita H. Study on the curing process of the receptor-type taste disorder. Bull OtoLaryngology Ni-hon Univ Faculty Med 1995;98:267-80.
24. Halyard YM, Jatoi A, Sloan AJ, et al. Does Zinc sulfate prevent therapy-induce taste alterations in head and neck cancer patients? Results of phase III double blind, placebo-controlled trial from the north central cancer treatment group (N01C4). Int J Radiat Oncol Bio Phys 2007; 67(5):1318-22.
25. Yoshida S, Endo S, Tomita H, et al. A double-bind study of therapeutic efficacy of Zinc gluconate on taste disorders. Auris Nasus Larynx 1991;18:153-61.
26. Silverman JE, Weber CW, Silverman S Jr, et al. Zinc supplementation and taste in head and neck cancer patients undergoing radiation therapy. J Oral Med 1983;38: 14-6.
27. Mossman K.L. Gustatory tissue injury in man: Radiation dose response relationships and mechanisms of taste loss. Br. J. Cancer 1986;53(Suppl.VII):9-11.

THE ASEAN JOURNAL OF RADIOLOGY 2012: 18(2): 108-117

Original Article

Added Value of SPECT Fused with CT in Assessing Single Equivocal Bone Lesion on Planar Scintigraphy

Arpakorn Kositwattanarerk, MD.[1] Warapat Virayavanich, MD.[2]
Chirawat Utamakul, MD., Chanika Sritara, MD. MSc.[1]

[1] Division of Nuclear Medicine Department of Radiology, [2] Department of Radiology, Faculty of Medicine, Ramathibodi Hospital, Mahidol University, Bangkok, Thailand

Abstract

Objective: The aim of this study was to evaluate the diagnostic value of fused single photon emission computed tomography (SPECT) and 16-slices multi-detector computed tomography (CT) obtained from separate machines in patient with single equivocal bone lesion on planar ^{99m}Tc-MDP bone scan.

Material and methods: All patients with single equivocal lesion seen on planar bone scintigraphy during June 2007 to Dec 2008 were sent for SPECT/CT. SPECT and CT were independently evaluated by two nuclear medicine physicians and a radiologist, each of whom was not aware of the results obtained through other imaging modalities. Subsequently, the specialist from both modalities interpreted the fused images by consensus. Pathological result or a 3-year follow-up was considered to be reference standard.

Results: There were 25 patients. Ten of them were male. The mean age was 61±14 years (age range 41-82 year). All of them have history of cancer. Sensitivity, specificity and overall accuracy of SPECT/CT were 60%, 100% and 84%, respectively. SPECT/CT increased reader's confidence in most cases. Only 1 patient has pathologically proved bony metastasis. Diagnosis of bony metastasis in the rest of the patients was done by follow-up clinical and imaging.

Conclusion: SPECT/CT fusion is a useful technique to evaluate single equivocal bone lesion. It increases reader's confidence and specificity of the test. However, further investigation with larger number of patients may be warranted.

Keywords: SPECT/CT, single equivocal bone lesion

Introduction

Despite new procedures have recently been developed for bone imaging, bone scan still plays a major role in the diagnosis of bone lesions of all kinds. Bone scan has proven to be highly sensitive, particularly in cancer patients suspected of having bone metastases.[1] Bone scan has the advantage of revealing metastases considerably earlier than radiographs because of the increased bone turnover caused by tumor growth. Bone scan is wildly available, well-established clinical experiences with modest efficacy in many types of cancer. Bone scan is not specific for malignancy. Increased uptake in bone scan also occurs in many benign conditions such as fracture or reflex sympathetic dystrophy.

As compared with planar scintigraphy, single photon emission computed tomography (SPECT) increases image contrast and improves lesion detection and localization.[2-6] However, SPECT still lacks anatomical detail. This is a significant drawback because further classification as benignity or malignancy is often based on the precise location of a lesion. On the other hand, structural changes shown on radiography are often difficult to assess without corresponding functional information.

Hence, combining both functional (SPECT) and anatomic data (CT) improves diagnostic accuracy and lesion characterization.[7,8] SPECT/CT promises to overcome the insufficient specificity of planar scintigraphy and SPECT alone. Ramathibodi Hospital does not have state-of-the-art SPECT/CT machine. Ramathibodi Hospital has separately SPECT and CT machines.

Thus, the purpose of this study was to evaluate prospectively if there is additional diagnostic value in fused SPECT and CT images for the assessment of single equivocal bone lesion on planar scintigraphy in Ramathibodi Hospital's patient.

Material and methods

Patients: All consecutive patients with single equivocal abnormal radiotracer uptake on planar bone scintigraphy during June 2007- Dec 2008 were enrolled in this prospective study. The study was approved by ethic committee on human rights related to researchers involving human subjects. Faculty of Medicine, Ramathibodi Hospital, Mahidol University. Written informed consent to add CT acquisition to the bone scan was performed in all patients.

^{99m}Tc-MDP planar scintigraphy: Whole body bone planar scintigraphy was acquired approximately at 2 hours after injection of 20 mCi of ^{99m}Tc-MDP using a dual-head gamma camera (Philips, FORTE, ADAC laboratory). Parallel-hole, low energy, high resolution collimator with a 20% window center at 140 KeV peak were used to obtain planar image in a continuous mode. Patients were asked to void before initiation of planar scintigraphy. Patients were lying in supine position.

SPECT images: SPECT images were acquired and processed using same dual- head gamma camera. Image setting was acquired as follows: 180° acquisition, 32 projections and 30 seconds per projection. No attenuation or scatter correction was acquired.

CT images: non-contrast CT scan using 16 slices CT scan (Philips MX 8000 CT scanner) was acquired at the area of equivocal lesion seen on planar bone scan. The acquisition parameters were used as follows: 120 kV 200 mAs and 5-mm reconstruction.

SPECT and CT machines were located separately. External markers for both SPECT and CT

were placed on patient's skin. SPECT/CT fusion images were obtained using software image fusion.

Attending nuclear medicine physician reviewed planar bone scintigraphy immediately after acquisition. SPECT/CT was requested in patient with single equivocal bone lesion seen in planar scintigraphy.

Image interpretation

In the first phase of image analysis, SPECT and CT were independently evaluated by two nuclear medicine physicians and one radiologist, each of whom was not aware of the results obtained through other imaging modalities. Subsequently, the specialist of both modalities interpreted the fused images by consensus.

The criteria to classify a focal bone lesion as benignity or malignancy for SPECT images depend on lesion location. At the spine, the lesion involving vertebral body or pedicle is typical for metastatic disease while lesion at the joints and endplates was benign. Lesion at pelvis was considered benign if it involved joint. Sternal lesion was interpreted as malignant if it involved manubrium and/or body of sternum. Involving sternoclavicular joint was considered benign.

Additional criteria for the CT part of the fused SPECT and CT interpretation to be considered malignant was if there were osteoblastic/ osteolytic lesions, or bone lesion with associated soft tissue mass. Sclerotic lesions with spondylophytes and disk space narrowing were considered benign, and so were lesion in the subchrondral region of a joint together with joint space narrowing, subchondral bone cysts and osteophytes. Readers were asked that whether SPECT/CT images increased reader's confidence of image interpretation.

Pathological result was considered to be a reference standard. If pathological result was not available, at least 3-year clinical and imaging follow-up was acceptable as a reference standard. Clinical follow-up data were obtained by reviewing patient's hospital charts. All of the follow-up images were reviewed by experienced radiologist to confirm the presence or absence of bony metastasis.

Results

From June 2007 - Dec 2008, twenty five patients underwent SPECT/CT due to single equivocal finding lesion seen on planar scintigraphy. Ten of them were male and 15 of them were female. The mean age of patients was 61±14 years (age range 41-82 year). All patients had underlying cancer. Twelve patients (48%) had bone pain while the rest of the patients were sent for metastatic work up without any symptom.

Primary cancer was classified as follows: breast (n=11), prostate (n=4), lung (n=3), bladder (n=2), sarcoma (n=2), GI malignancy (n=1), hepatoma (n=1) and gynecologic malignancy (n=1).

Most common sites of equivocal lesions on planar bone scintigraphy were at lumbar spine (n=12), pelvic bone and sacrum (n=6).

In the group of patients with bone pain (n=12), the location of bone pain was classified as follows: lumbar spine (n=9), cervical spine (n=1), thoracic spine (n=1) and lower extremities (n=1). Nine patients have abnormally increased uptake at the same region of clinical bone pain. Two patients developed bone metastasis during follow-up.

Sensitivity, specificity and overall accuracy of SPECT/CT were 60%, 100% and 84%, respectively. In most cases, SPECT/CT did not change diagno-

sis compared with SPECT or CT alone, but it increased reader's confidence (72%).

Tissue diagnosis was available in only 1 patient. Bone scan picture of this patient was demonstrated in Fig 1. A 43-year-old female had history of cervical cancer treated with radiation therapy for 18 months. She presented with low back pain, which was suspected to be due to bony metastasis. SPECT/CT images showed increased uptake at L4 vertebra, corresponding to an area of bone destruction with suspected soft tissue invasion into spinal canal. Bone metastasis was suggested. MRI was subsequently done 1 month after bone scan. MRI (Fig 2) demonstrated evidence of lower L4 endplate irregularity and L4+L5 destruction with adjacent left paravertebral mass that were suggestive of liquefied abscess in the left psoas muscle. Infectious process was considered. Spinal metastasis with necrotic tumor was in the differential diagnosis. Two weeks later, the patient underwent fluoro-guided biopsy which proved to be metastatic squamous cell carcinoma.

Diagnosis of bony metastasis in the rest of the patients was done by following up clinical and imaging. Timing for follow-up was at least 3 years.

For the patients who were reported bone metastasis from SPECT/CT images, follow- up clinical and imaging confirmed bone metastasis in all patients. However, a few cases of reported benign finding on SPECT/CT scan proved to be bone metastasis during the 3-year follow-up period. The authors demonstrated an example of the case in Fig 3. An 80-year-old male had a history of prostatic cancer for a year. He refused to do surgery. Only hormonal treatment was ordered. He presented with back pain. His PSA level was 0.621 ng/ml. Increased uptake at L2 vertebra was corresponding with an area of well-defined osteoblastic lesion seen on CT scan (Fig 3). Benign process was suggested. Three months later, the patient underwent MRI lumbosacral spine, which revealed the ill- defined, partial enhancing hypo-hypersignal T1/ T2 lesion at mid and right-sided L2 vertebral body, suggestive of marrow infiltrative process from metastasis.

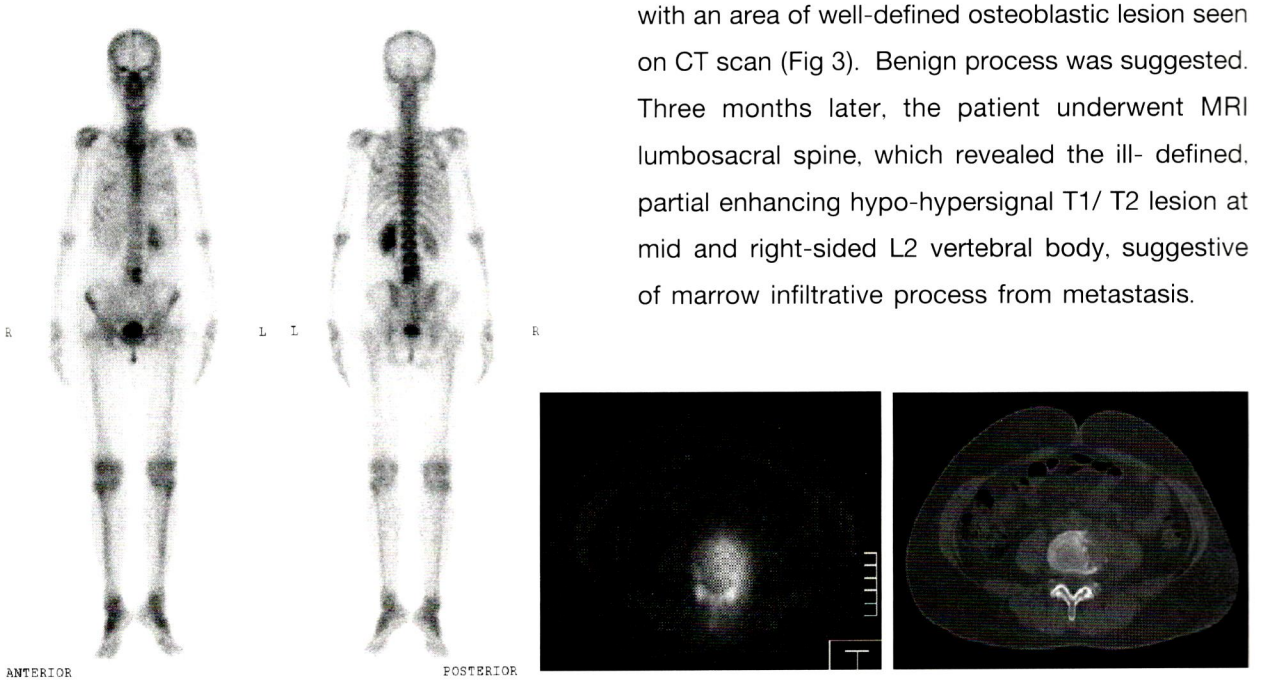

Fig.1 Planar bone scintigraphy, axial SPECT/CT and plain CT of a 43-year-old female who had history of cervical cancer and back pain for 6 months. Increased uptake in an area of bone destruction in the left-sided L4 was seen. Soft tissue invasion into spinal canal was suspected. Bone metastasis was suggested.

Fig.2 MRI lumbosacral spine (T2, T1, T1FS and T1+C) was done at 2 months later. Evidence of lower L4 end plate irregularity and L4+L5 destruction with adjacent left paravertebral mass were suggestive of liquefied abscess in the left psoas muscle. Infectious process was considered. Spine metastasis with necrotic tumor was in the differential diagnosis. The patient underwent fluoro-guided biopsy which proved to be metastasis SCCA.

The authors demonstrated another interesting case in Fig 4-5. A 60-year-old male had a history of bladder cancer S/P radical cystectomy and ileal conduit. There was increased uptake in the right-sided pelvic bone on planar image (Fig 4), which could be due to urine activity in ileal conduit or bone lesion. SPECT/CT images (Fig 4) demonstrated radiotracer activity in the ileal conduit, outside normal bony structure. No evidence of osteoblastic or osteolytic bone lesion was seen in plain CT scan. SPECT/CT in this case excluded the presence of bone metastasis in pelvic bone at that time, although interval follow up bone scan 2 years later (Fig 5) found multiple bony metastases.

The authors demonstrated an example of the false negative case in Fig 6-7. A 36-year-old female with a history of breast cancer treated with lumpectomy and chemotherapy for 2 years, presented with back pain. Previous bone scan was negative. SPECT/CT images (Fig 6) revealed increased uptake at superior portion of the left sacrum, which was corresponding with secondary degenerative change from left-sided L5 sacralization. Degenerative change was interpreted. However, bone metastasis was confirmed by plain radiograph and CT scan 2 years later (Fig 7).

Discussion

Bone scan is very useful in cancer patients who are suspected to have bone metastasis. It provides whole body imaging, high sensitivity with modest specificity. Characterization of single equivocal bone lesion as benign or malignant is an important finding with regard to tumor staging or restaging.

SPECT/CT increased both sensitivity and specificity of the test.[9,10] SPECT can distinguish the precise location (i.e. lesion in vertebral body or joint) while plain CT can give more anatomical information such as osteoblastic/ lytic lesion. SPECT/CT

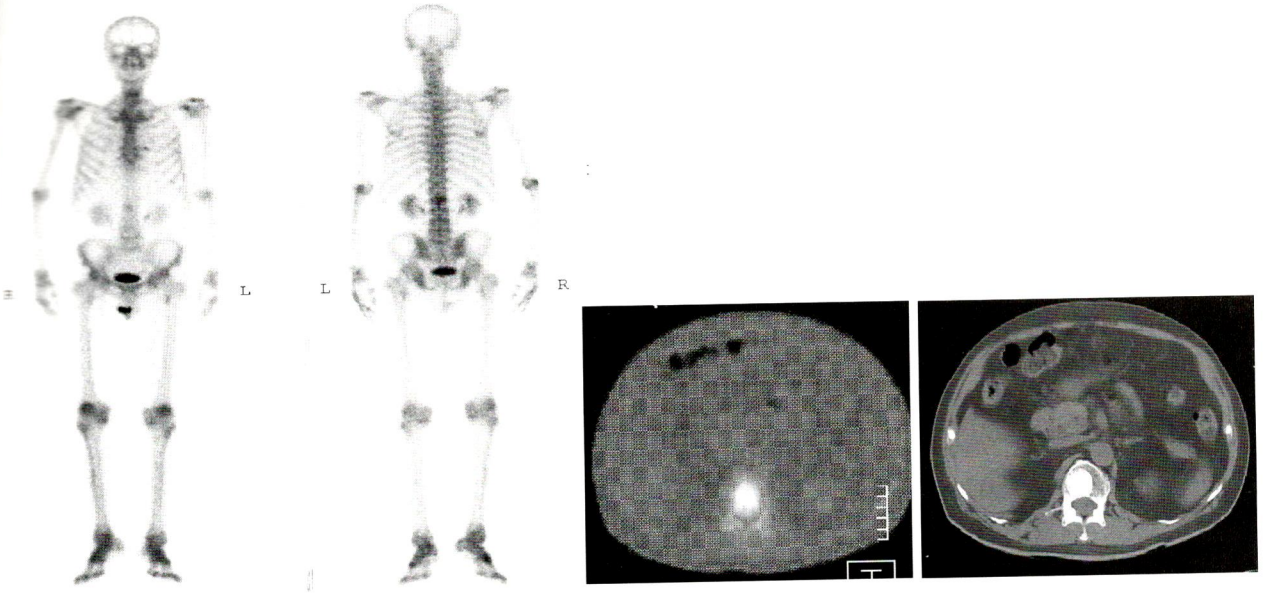

Fig.3 Planar bone scintigraphy, axial SPECT/CT and plain CT of an 80-year-old male with prostate cancer who presented with back pain. There is increased uptake at a well-defined osteoblastic lesion in L2 vertebra. Benign process was suggested. However, MRI lumbosacral spine at 6 months later showed L2 metastasis.

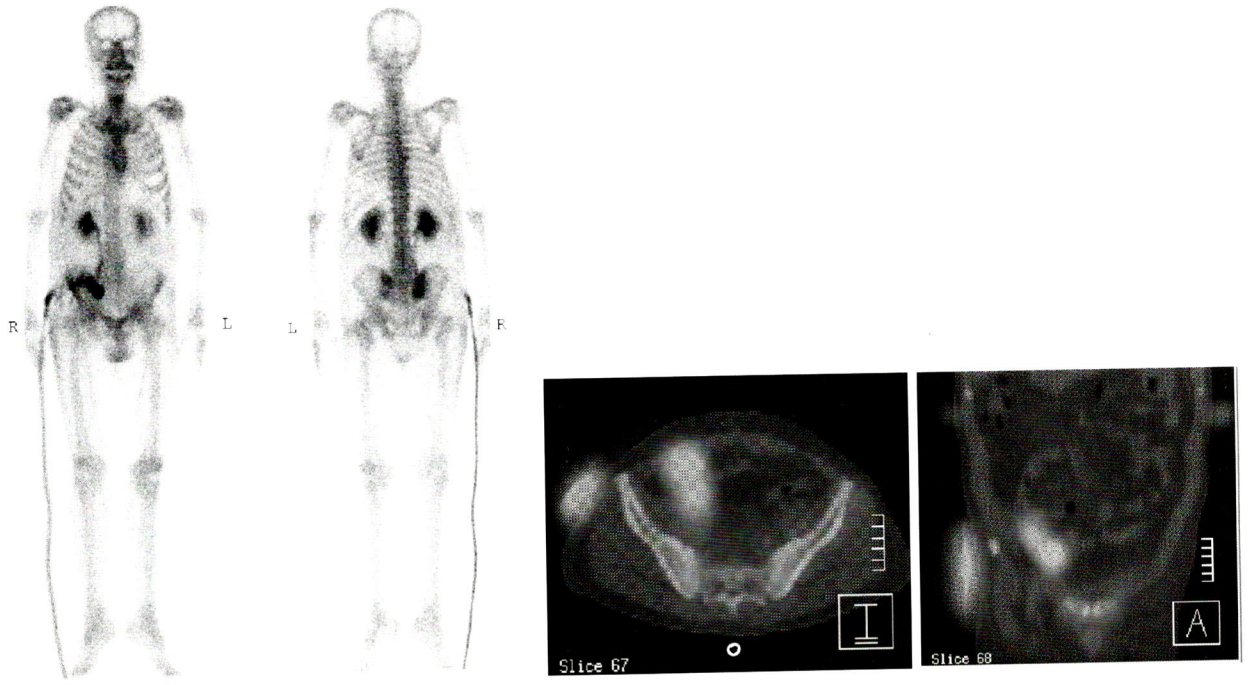

Fig.4 Planar bone scan, axial and coronal SPECT/CT images of a 60-year-old male with bladder cancer revealed increased uptake in the right-sided pelvic bone, which could be due to urine activity in ileal conduit or true bone lesion. SPECT/CT images demonstrated radiotracer activity in the ileal conduit, outside normal bony structure. No evidence of osteoblastic or osteolytic bone lesion was seen in plain CT scan.

Fig.5 A follow up bone scan of this patient after chemotherapy was done at 1 year later. Multiple bone metastases were obviously seen in this bone scan.

improves diagnostic confidence and makes a definitive diagnosis in most cases. Franc BL. et al.[11] recently reported the sensitivity, specificity and accuracy of SPECT/CT to be 90.9%, 85.9% and 87%, respectively. These values did not differ significantly from those obtained from SPECT alone. SPECT/CT should be used on a patient-by-patient basis. However, in that article, most of their patients (72%) were non oncologic patient while all of our patients had history of cancer.

Almost half of our patients (11/25) had underlying breast cancer, which is one of the most common cancer in Thailand. Sharma P. et al[12] summarized that SPECT/CT is better than planar scintigraphy and SPECT alone for characterizing equivocal bone lesion in patient with breast cancer and can have significant impact on patient management. Differentiation between benign and malignant lesion in single lesion, especially in axial skeleton, is critical. SPECT/CT decreased the number of equivocal finding in planar bone scan while these bone lesions located in spine[13,14] as well as in skull[15].

Ndlovu X. et al.[16] reported that SPECT/CT significantly outperformed SPECT alone for the interpretation of skeletal lesions in patient undergoing bone scanning for metastases. SPECT/CT resulted in a significant reduction of equivocal findings. Iqbal B et al.[14] showed that specificity of bone scan was excellent (100%) for characterizing solitary spine lesion. However, sensitivity of planar bone scan was extremely low (6.1%), which can be significantly increased (to 78.8%) after the addition of SPECT/CT. Acquiring SPECT images in all patients are unnecessary and time consuming. In this article, the authors selected patients with single equivocal bone lesion to acquire SPECT/CT. Differentiation between benign and malignant lesion may affect cancer staging as well as further treatment planning. The authors didn't compare planar bone scan with SPECT and SPECT/CT because it has been clearly demonstrated in previous reports that SPECT/CT is better than both planar and SPECT

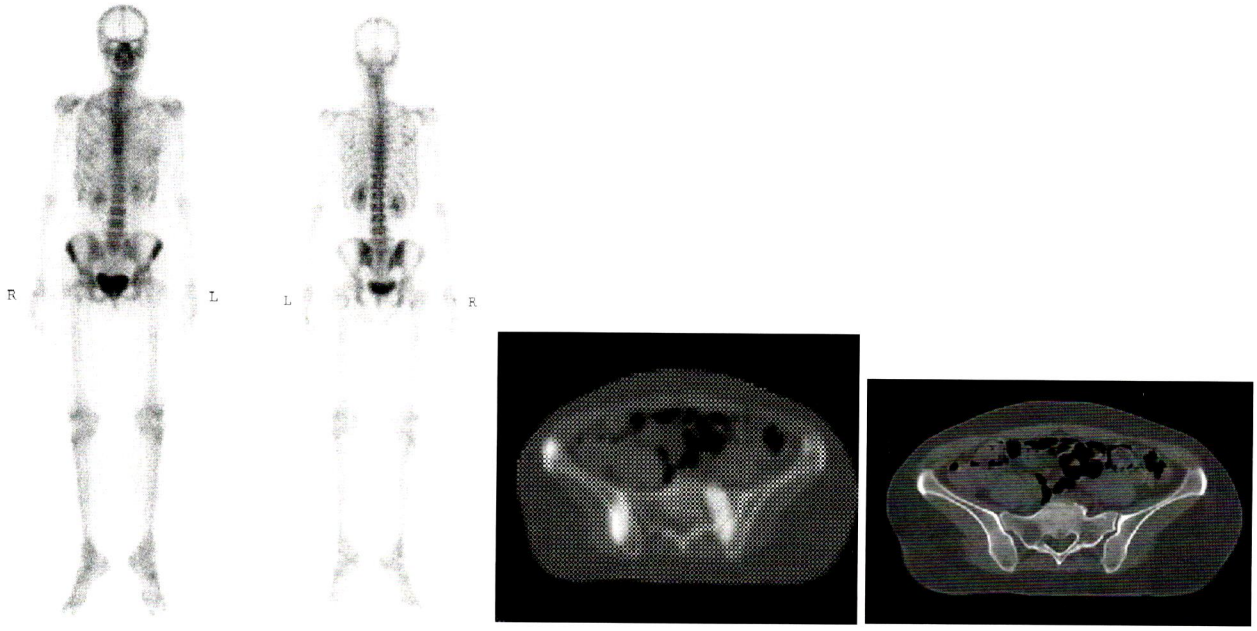

Fig.6 Planar bone scintigraphy, axial SPECT/CT and plain CT of a 36-year-old female, who had a history of left breast cancer status post complete treatment for 2 years. Previous bone scan was negative. She presented with back pain. Planar bone scan showed increased uptake focus in the right SI joint. SPECT/CT image showed increased uptake in the sacralization of left-sided L5 vertebra with secondary degenerative change at transverse process-sacral junction. Degenerative change was suggested.

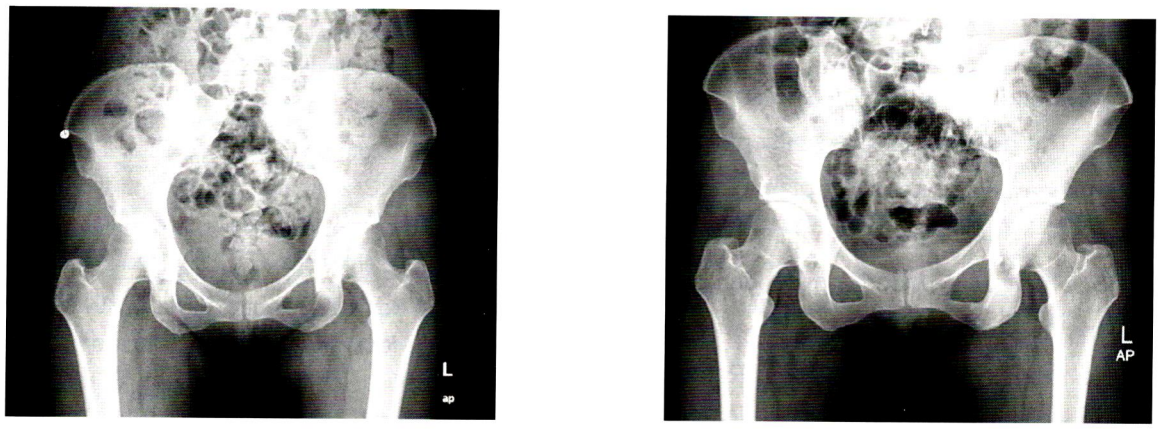

A. B.

Fig.7 Follow up images were done at 18 months (A.) and 24 months. (B.) The first follow up image was unremarkable. However, sclerotic change of the left-sided sacrum and left inferior pubic ramus was clearly identified in Fig B. Bone metastasis was suggested. Multiple bone metastases in vertebrae and pelvis were confirmed in CT scan whole abdomen, which was obtained 2 months later.

images. Most of previous articles acquired SPECT/CT using the same machine. Utsunomiya el al.[17] showed that analysis of simultaneously fused SPECT/CT images improve reviewers' confident of differentiating malignant from benign lesions in a compared with a side-by-side viewing of 2 sets of images (SPECT and CT). In Ramathobodi Hospital setting, the authors acquired SPECT and CT separately using dual head gamma camera (FORTE, Philips) and Philips MX 8000 CT scanner, respectively. Then software image fusion was acquired. Data from this setting is still limited. Strobel et al.[18] compared the usage of planar bone scan, SPECT and SPECT/CT in order to characterize focal bone lesions in the axial skeleton. They performed bone SPECT with dual head gamma camera and CT with a standalone 64-MDCT scanner. Then digital software fusion was obtained. Sensitivity and specificity for differentiation benign and malignant lesions were 82% and 94% for planar bone scan, 91% and 94% for SPECT, and 100% and 100% for SPECT/CT. Sensitivity, specificity and overall accuracy of SPECT-CT in our setting were 60%, 100% and 84%, respectively.

Limitation of this study was the small number of patients. The authors selected patients who had single equivocal lesion seen on planar bone scan and didn't have any correlative imaging before bone scan. For patient with underlying cancer and multiple lesions seen on planar bone scan, there is a high probability of bony metastases. Pathological result was not available in most cases. Since most bone scan results were interpreted as benign etiology, it was impractical and unethical to perform surgery or biopsy in these patients. Furthermore, the authors did SPECT and CT separately from different machine. SPECT/CT fusion was done by a software fusion using external marker. Incorrect lesion localization was possible.

SPECT/CT fusion is a useful technique in evaluating single equivocal bone lesion. It increases reader's confidence and the test's specificity. However, further investigation with a larger number of patients may be warranted.

References

1. Love C, Din AS, Tomas MB, Kalapparambath TP, Palestro CJ. Radionuclide bone imaging: an illustrative review. Radiographics 2003;23(2):341-58. Epub 2003/03/18.
2. Savelli G, Chiti A, Grasselli G, Maccauro M, Rodari M, Bombardieri E. The role of bone SPET study in diagnosis of single vertebral metastases. Anticancer research 2000;20(2B):1115-20.
3. Even-Sapir E, Martin RH, Barnes DC, Pringle CR, Iles SE, Mitchell MJ. Role of SPECT in differentiating malignant from benign lesions in the lower thoracic and lumbar vertebrae. Radiology 1993;187(1):193-8.
4. Ryan PJ, Evans PA, Gibson T, Fogelman I. Chronic low back pain: comparison of bone SPECT with radiography and CT. Radiology 1992;182(3):849-54.
5. De Maeseneer M, Lenchik L, Everaert H, Marcelis S, Bossuyt A, Osteaux M, et al. Evaluation of lower back pain with bone scintigraphy and SPECT. Radiographics 1999;19(4):901-12; discussion 12-4.
6. Savelli G, Maffioli L, Maccauro M, De Deckere E, Bombardieri E. Bone scintigraphy and the added value of SPECT (single photon emission tomography) in detecting skeletal lesions. Q J Nucl Med 2001;45(1):27-37.
7. Romer W, Nomayr A, Uder M, Bautz W, Kuwert T. SPECT-guided CT for evaluating foci of increased bone metabolism classified as indeterminate on SPECT in cancer patients. J Nucl Med 2006;47(7):1102-6.
8. Roach PJ, Schembri GP, Ho Shon IA, Bailey EA, Bailey DL. SPECT/CT imaging using a spiral CT scanner for anatomical localization: Impact on diagnostic accuracy and reporter confidence in clinical practice. Nuclear medicine communications 2006;27(12):977-87.

9. Horger M, Bares R. The role of single-photon emission computed tomography/computed tomography in benign and malignant bone disease. Seminars in nuclear medicine 2006;36(4):286-94.
10. Horger M, Eschmann SM, Pfannenberg C, Vonthein R, Besenfelder H, Claussen CD, et al. Evaluation of combined transmission and emission tomography for classification of skeletal lesions. Ajr 2004;183(3):655-61.
11. Franc BL, Myers R, Pounds TR, Bolton G, Conte F, Bartheld M, et al. Clinical utility of SPECT-(low-dose)CT versus SPECT alone in patients presenting for bone scintigraphy. Clinical nuclear medicine 2012;37(1):26-34. Epub 2011/12/14.
12. Sharma P, Kumar R, Singh H, Bal C, Julka PK, Thulkar S, et al. Indeterminate lesions on planar bone scintigraphy in lung cancer patients: SPECT, CT or SPECT-CT? Skeletal radiology 2011. Epub 2011/10/18.
13. Zhang Y, Shi H, Gu Y, Xiu Y, Li B, Zhu W, et al. Differential diagnostic value of single-photon emission computed tomography/spiral computed tomography with Tc-99m-methylene diphosphonate in patients with spinal lesions. Nuclear medicine communications 2011;32(12):1194-200. Epub 2011/09/22.
14. Iqbal B, Currie GM, Wheat JM, Raza H, Kiat H. The incremental value of SPECT/CT in characterizing solitary spine lesions. Journal of nuclear medicine technology 2011;39(3):201-7. Epub 2011/07/29.
15. Gayed IW, Kim EE, Awad J, Joseph U, Wan D, John S. The value of fused SPECT/CT in the evaluation of solitary skull lesion. Clinical nuclear medicine 2011;36(7):538-41. Epub 2011/06/04.
16. Ndlovu X, George R, Ellmann A, Warwick J. Should SPECT-CT replace SPECT for the evaluation of equivocal bone scan lesions in patients with underlying malignancies? Nuclear medicine communications 2010;31(7):659-65. Epub 2010/04/17.
17. Utsunomiya D, Shiraishi S, Imuta M, Tomiguchi S, Kawanaka K, Morishita S, et al. Added value of SPECT/CT fusion in assessing suspected bone metastasis: comparison with scintigraphy alone and nonfused scintigraphy and CT. Radiology 2006;238(1):264-71. Epub 2005/11/24.
18. Strobel K, Burger C, Seifert B, Husarik DB, Soyka JD, Hany TF. Characterization of focal bone lesions in the axial skeleton: performance of planar bone scintigraphy compared with SPECT and SPECT fused with CT. Ajr 2007;188(5):W467-74.

THE ASEAN JOURNAL OF RADIOLOGY 2012: 18(2): 118-122

Original Article

Radiation from an Admitted Thyroid Cancer Patient with High Dose I-131 Treatment in Related Hospitalized Area and Exposure to Associated Personnel in Ramathibodi's New Inpatient Unit

Wirote Changmuang[1], Wichana Chamroonrat[1*], Arpakorn Kositwattanarerk[1], Siripong Vittayachokkitikhun[1], Kittiphong Thongklam[1], Krisanat Chuamsaamarkkee[1], Natthaporn Kumwang[2], Chanika Sritara[1]

[1] Division of Nuclear Medicine, Department of Radiology, Faculty of Medicine Ramathibodi hospital, Mahidol University,

[2] Thailand Institute of Nuclear Technology

Abstract

Purpose: After an administration of high dose I-131 in differentiated thyroid cancer, patients are potential sources of radiation. The aim of this study is to clarify radiation in the admitting room and associated surrounding of Ramathibodi's new inpatient unit during hospitalization of a high dose I-131 treated thyroid cancer patient as well as radiation exposure to associated personnel.

Materials and Methods: The radiation dose rate was measured using optically stimulated luminescence dosimeter (OSL) (Al_2O_3:C) which placed and interpreted in 22 different locations within and adjacent the admitting room prior and during admission of a high dose I-131 treated patient. Collections of the room air were performed using gamma counters, compared 2 durations with and without the occupied patient in the room. The direct exposure was recorded by digital semiconductor pocket dosimeters, which were carried by patient's caregivers of every shift, namely morning, evening and night ones.

Results and discussions: The locations with the high radiation dose rate were around the patient bed between 11.86-51.41 μSv/h, which are expected. While room occupied, all location outside the admitted room was within background ranges (<1 μSv/h). Radioiodine concentrations in the room air were also within safety ranges. Calculated exposure to related personnel and public individual are within safety limits.

Conclusions: Our results provided assurance in using high dose radioiodine therapy in Ramathibodi's new inpatient unit for both public and related health care providers.

** Correspondence : Wichana Chamroonrat, MD.*

270 Rama VI Rd., Ratchathevi, Bangkok 10400 Thailand (Email : wichana-cha@mahidol.ac.th)

Introduction

High dose radioiodine (I-131 >1.1 GBq or 30 mCi) has been widely used in the standard treatment of differentiated thyroid cancer. After administration of the I-131 dose, patients are potential sources of radiation. According to International Atomic Energy Agency (IAEA), patients should be isolated which usually refer to admission in the hospital and discharged when theirs irradiation are less than the guidance level[1].

The International Commission of Radiological Protection (ICRP) has recommended a yearly radiation constraint of 1 mSv and 20 mSv for general population and radiation workers, respectively[2]. Vice versa, The Office of Atomic for Peace (OAP) has recommended an hourly radiation limit of 1 μSv and 10 μSv for public and occupational exposure, respectively[3]. Both recommendations are being followed in Thailand.

I-131 emits gamma and beta radiations. Although, gamma and beta emissions are characteristically different, both could be posed as sources of external radiation exposure to others. In addition, I-131 could be volatile, especially in a free form or acidic solution, and possibly a source of internal radiation exposure. The physical haft-life of I-131 is 8.04 days. Our prior study[4] showed effective half-life of 26.2±10.8 hours in high dose I-131 treated thyroid cancer patients. Therefore, our patients usually have one to two overnight stays in the hospital.

Well-known dosimeters for absorbed radiation dose rates include optically stimulated luminescence dosimeter (OSL) and thermoluminescent dosimeter (TLD). These dosimeters are highly sensitive with a dose range from 1 μSv to 10 Sv[5], which is particularly suitable for individual monitoring in low-radiation environment.

High dose I-131 treatment in differentiated thyroid cancer has been performed for several decades in Ramathibodi hospital. Currently, a capsule form of I-131 is used in almost all cases. However, the treatment is relatively new to Somdech Phra Debaratana Medical Center, the most recent facility in Ramathibodi hospital. Prior to high dose radionuclide treatment in the new inpatient facility, courses including basic radiation knowledge, radiation pro tection and certain radionuclide treatments were held. However, there have been some concerns in the unfamiliar territory, especially safety issues, which lead into this study.

The study aim is to clarify the radiation in the admitting room and associated surrounding of Ramathibodi's new inpatient unit during hospitalization of a high dose I-131 treated patient as well as exposure to associated personnel.

Materials and Medthods

Radiation measuring by location

The measurement was performed for 2 durations, prior and in-between admission of a high dose I-131 treated patient. The patient is a 24-year-old female with papillary thyroid cancer. The dose of I-131 treatment was 150 mCi (5550 MBq). She had an uneventful hospitalization of 2 overnight stays. The admitting room was 7211 in Somdech Phra Debaratana Medical Center (SPDMC), Ramathibodi Hospital (Figure 1).

1. InLight® OSL (Al_2O_3:C) dosimeters for radiation dose rate

A set of twenty-two OSL dosimeters was placed within the admitting room and surrounding in the locations shown in Figure 1. The placement was done twice. Each placement continued for 48 hours which included the whole admission. These

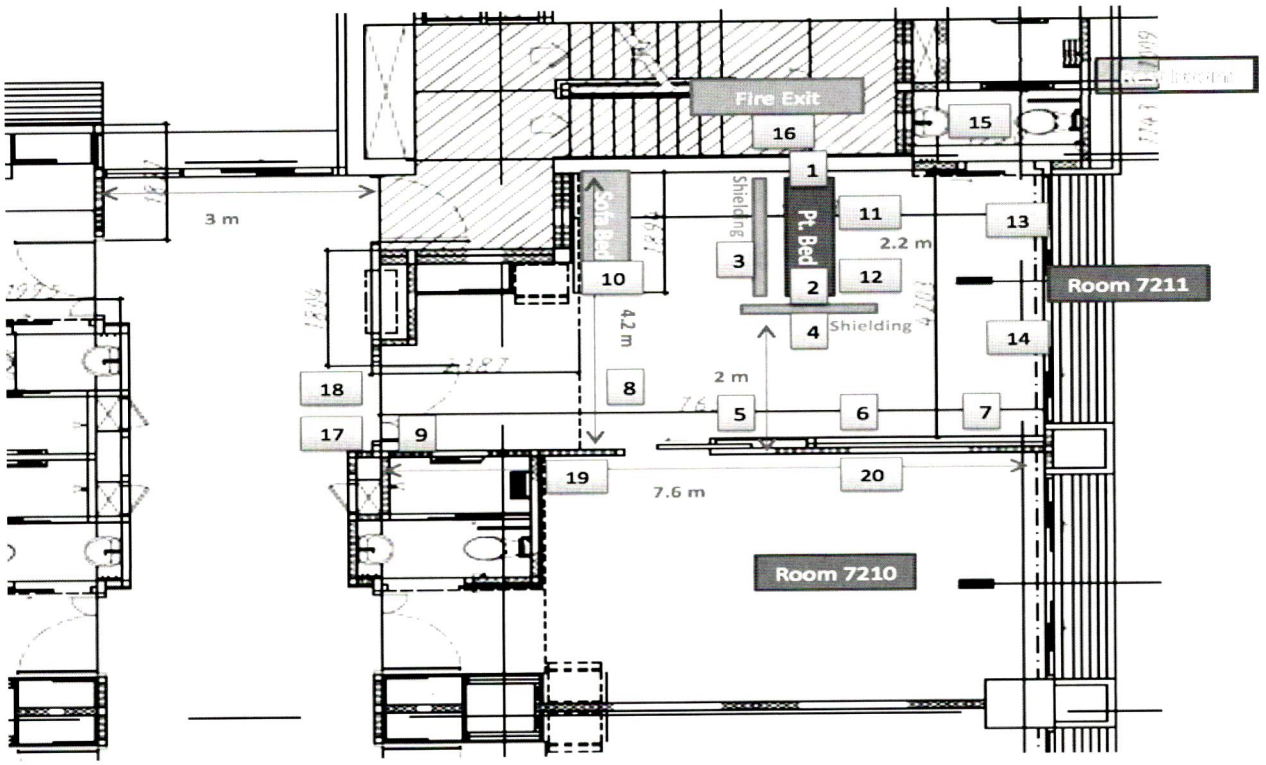

Fig.1 Blueprint of the assigned admitting room and surrounding areas with locations of OSL dosimeters.

OSL dosimeters were calibrated and read out with microStar® Dosimetry Reader, LANDAUER®, performed by Nuclear Technology service Center, Thailand Institute of Nuclear Technology.

2. SENSDYNE® DOX II air simpler for I-131 concentration in room air

Air at the top of patient bed was sampling in the simpler. The collected air flew through the simpler of rate at 3 liters per minute for 3 hours prior the admission. The similar sample with the occupied room was collected for 24 hours. The simples were subsequently measured with gamma probe, CAPTUS 3000®, CAPINTEC. The generic equation for the I-131 concentration in room air could be shown as:

Activity (Bq/m^3) = (net cps)/(efficiency x air volume)

Radiation measuring by individual personnel

Digital semiconductor pocket dosimeters (ALOKA model PDM-112) was carried and recorded by patient's caregivers of every shift, namely morning, evening and night ones.

Results and Discussions

Prior to admission of a thyroid cancer patient with high dose I-131 treatment, OSLs in all location revealed background level of radiation dose rate (<1 μSv/hr).

After an admission of a treated thyroid cancer patient with high dose of I-131, another set of OSLs was interpreted as in Table 1. Radiation dose rate of all location outside the patient room remained as background level, while the rate ranged between background levels to 51.41 μSv/h within patient room.

Table 1 Radiation dose rate (μSv/h) inside and surrounding treatment I-131 patient room.

NO.	Location of OSL	Radiation dose rate (μSv/h)
	Inside patient's room	
1	Top of patient bed	25.67
2	End of patient bed	13.11
3	Right hand of patient bed, Behind lead barrier	Bg
4	End of patient bed, Behind lead barrier	Bg
5	Wall to contact other room, right	1.11
6	Wall to contact other room, center	Bg
7	Wall to contact other room, left	1.73
8	Near a door	1.04
9	In front of exit door	Bg
10	Sofa bed	5.34
11	Under patient bed, top	51.41
12	Under patient bed, end	11.86
13	Window 1	7.35
14	Window 2	5.62
15	Restroom	2.71
	Outside patient's room	
16	Fire exit	Bg
17	Corridor 1	Bg
18	Corridor 2	Bg
19	Room number 7210, left	Bg
20	Room number 7210, right	Bg
21	8^{th} floor, patient bed	Bg
22	8^{th} floor, toilet	Bg

Bg is background radiation (< 1 μSv/h)

Four locations with radiation dose rate more than 10 μSv/h (less than 10 μSv/h consider acceptable level for radiation worker) included location numbers 1, 2, 11 and 12 which are all around the patient's bed with 25.67, 13.11, 51.41 and 11.86 μSv/h, respectively. These numbers are expected because the patient should be in bed about or at least half of the time she admitted including sleeping. One main general instruction to patients with high-dose radionuclide treatment during admission is to remain within bed behind lead barriers or shielding if having any visitor including relative, friend and health care personnel. However, once being alone, the patient as a movable radiation source probably ambulated and entertained herself within the room. Therefore, the following locations with radiation dose rate 5-10 μSv/h may imply that she rested in the sofa bed (location number 10), sat or ate at the dining table by the window (location numbers 13-14) or just looked for scenery outside the hospital room. The rest of the location including restroom revealed radiation dose rate less than 5 μSv/h.

Our result was similar to the study of Abu-Khaled and et al[6]. They measured the radiation exposure in surrounding the room of patients treated with I-131 using TLD-200. The radiation dose rates measured was 25.78±Sv/h at the patient bed; 10.78 μSv/h in the bathroom; and 1.31 at the visitor chair. The radiation dose rates at the outside of the external door and public corridor were between 0.14 and 0.10 μSv/h, respectively.

Radioiodine concentration in the room air was 1.21 and 1.36 Bq/m^3 per week, before and during admission, respectively (acceptable limit 8.33 Bq/m^3 per week)[7].

The radiation doses to the nurse who cared the patient were recorded by using digital semi-conductor pocket dosimeter. There are three nurse shifts each day namely morning, evening and night ones. Each shift lasts about 8 hours and the duty usually includes general patient visit for any symptom or need, food tray delivery and collection, vital signs and intake/output checks. Individual nurse of each shift who cared for the patient carried a pocket dosimeter which reported 0-1 μSv/shift for the entire admission.

Conclusions

Having a new inpatient facility, safety concern was raised when radiation involved. This study provided assurance of radiation safety for both public and related health care providers with a hospitalized patient receiving high dose radioiodine therapy following standard guidelines from ICRP and OAP organizations.

In addition, pattern of radiation dose rate in different locations within the admitted room implied patient behavior during isolation.

Acknowledgment

The authors wish to thank the Nuclear Technology service Center, Thailand Institute of Nuclear Technology for the OSL interpretation.

The authors appreciate all guidance and collaborations from Prof. Dr. Aram Rojanasakul and SPDMC staffs in this study.

References

1. IAEA Safety Reports Series No. 40 (2005). Applying radiation safety standards in nuclear medicine. International Atomic Energy Agency Vienna.
2. International Commision on Radiological Protection (2004). Release of patients after radionuclide therapy with unsealed radionuclides. Publication 94, Elsevier, Oxford.
3. Nuclear Medicine Society, Medical Physicist Society and Office of Atoms for Peace (2006). Radiation Safety Management in Nuclear Medicine. The workshop at Office of Atoms for Peace, Thailand.
4. Changmuang W., Anongpornjossakul N., Thongklam K., Poonak K. and Toengkhuntod R. Evaluation of Dosimetric Parameters from Patients Based on Whole Body 131I Bio-Kinetic Clearance in Thyroid Cancer Therapy. Rama Med J 2012;35(1):42-47.
5. Govinda R., Joanna I. Radiation Monitoring Measurement. Review of Radiation Oncology Physics 85-102.
6. Abu-Khaled Y.S., Sandouqa A.S. and Haddadin I.M. Radiation Exposure From Radioactive Iodine I-131 In And Surrounding The Patients' Room. Radiat Prot Dosimetry 2009;135(1):64-68.
7. IAEA Basic Safety Standards No. RS-G-1.2 (1999). Assessment of Occupational Exposure Due to Intakes of Radionuclides. International Atomic Energy Agency Vienna.

THE ASEAN JOURNAL OF RADIOLOGY 2012: 18(2): 123-132 123

Original Article

Doxorubicin in the Treatment of Hepatocellular Carcinoma by Drug-eluting Bead Embolization: Initial Experience in Ramathibodi Hospital

Banjongsak Wedsart, MD., Jiemjit Tapaneeyakorn, MD., Tanapong Panpikoon, MD., Tharintorn Treesit, MD.

Division of Body Interventional Radiology, Department of Radiology, Ramathibodi Hospital, Mahidol University, Bangkok 10400, Thailand

Abstract

Introduction: We assessed the successful rate after Transarterial chemoembolization (TACE) with drug eluting beads (DEB; DC bead, Biocompatibles, Surrey, UK) for unresectable hepatocellular carcinoma (HCC). We also analyzed the factors affecting successful rate of DEB-TACE and its complications.

Materials and Methods: Of 10 consecutive patients with 13 unresectable HCC, 16 TACE were performed by using 50 mg Doxorubicin mixed with 300-500 mm DEB. The follow up CT or MRI 4 weeks after procedure was performed to evaluate the successful rate. If residual tumor appeared, follow-up embolization was performed.

Results: Among 10 patients with 13 HCC, 7 patients with 8 HCC were completely necrotic in single session without recurrence within 3 month follow-up study. All of them had single arterial feeder and 87.5% had tumor size smaller than 5 cm. The rest were completely necrotic in the 2nd and 3rd sessions. Of the 16 procedures, only one had severe complication, 4 had mild complication and 11 had no complication at all.

Conclusion: TACE with DEB had good successful rate for unresectable HCC with mild complication. Tumor size smaller than 5 cm and single tumor arterial feeder were significant factors affecting successful rate.

Introduction

Hepatocellular carcinoma (HCC) in men is the fifth most frequently diagnosed cancer worldwide but the second most frequent cause of cancer death. In women, it is the seventh most commonly diagnosed cancer and the sixth leading cause of cancer death[1]. Approximately three-fourth of cases occur in Asian countries because of a high prevalence of chronic infection with HBV. HCC is undoubtedly a great health threat in Asian region[2].

Transarterial chemoembolization (TACE) is targeted delivery of chemotherapeutic agents, usually mixed with Lipiodol followed by embolization or reduction in arterial flow using various types of particles, while sparing the surrounding liver parenchyma[3]. This combination of highly concentrated chemotherapy and arterial embolization may induce highly concentrated chemotherapy and ischemic damage on the tumor, which is likely to be synergistic in producing tumor necrosis[4].

To date, TACE is recommended by the Society of Interventional Radiology (SIR) as a first-line treatment for patients with inoperable, large/multifocal HCCs who do not have vascular invasion or extrahepatic spread. Selective TACE can be performed in early-stage patients in whom RFA is difficult to be performed because of tumor location or medical comorbidities[5].

The ideal TACE scheme should allow maximum and sustained concentration of chemotherapeutic agents within the tumor with minimal concentration of chemotherapeutic agents in peripheral blood combined with tumoral vessel obstruction[6].

Recently, embolic microspheres that have the ability to sequester doxorubicin hydrochloride from the solution and release it in a controlled and sustainable fashion were introduced for intra-arterial injection. The embolization particles are made from a unique drug-eluting technology i.e., doxorubicin-eluting beads (DEB) (Figure 1), based on a hydrogel that has modified with sulphonate group. These allow gradual release of chemotherapy over time, prolong the contact time between cancer cells and avoid damage of the hepatic microcirculation. Selective delivery of the loaded beads into the feeding arteries leads to vessel occlusion and ischemia, while doxorubicin is gradually released locally, leading to tumor necrosis[7-9].

In this study, the authors presented the results, including successful rate and complication, of early experience treating 13 inoperable HCCs in 10 patients using DEB-TACE.

Fig.1 Drug-eluting bead size 300-500 microns.

Material and Methods

Patients

The authors performed a retrospective study-based analysis of 10 patients with 13 unresectable HCC, treated with DEB-TACE in a single centre between January 2010 and June 2011. Following embolization, all patients had at least one follow-up

imaging with either multiphase CT or MRI. If residual tumor appeared, followed TACE was performed. Diagnosis of HCC was either confirmed by biopsy or based on radiological findings and alphafeto protein level according to European Association for the Study of Liver criteria (EASL criteria). According to the Barcelona Clinic Liver Cancer (BCLC) algorithm, TACE is widely accepted as the standard for allocating treatment in HCC patients, consequently the inclusion and exclusion criteria for DEB-TACE in this study are the same as for conventional TACE[10].

Embolization technique

All procedures were performed by interventional radiologists after patients had given their informed consents for the procedures. Celiac and hepatic arterial angiographies were performed prior to embolization to demonstrate the tumor feeding arteries, identify variation in the liver arterial supply and exclude portal venous shunting. The recommended dose range, suggested by the Precision study, is 25-37.5 mg of doxorubicin per ml of hydrated beads (50-150 mg/procedure/patient)[9,11]. In this study, the 2 ml of the 300-500 μm DEB were uploaded with 50 mg doxorubicin (Adriblastina; Farmitalia, Milan, Italy) in the vitro an hour and then aspirated into a syringe filled with non-ionic contrast medium (concentration 1:3) to ensure smooth catheter delivery. After selective or superselective catheterization into the distal portion of the tumor-feeding subsegmental artery was performed as selective as possible using 5 Fr diagnostic catheter (Chuang catheter or Cobra catheter) or 2-3 Fr coaxial microcatheter (Progreat, Terumo, Tokyo, Japan or Renegade, Boston Scientific, MA, USA), we slowly infused the loaded beads under fluoroscopic guidance. Additional 300-500 μm DEB could be used when needed to obtain complete obstruction of the tumor feeding arteries. Non-target embolization was avoided by loaded bead injection distal to the origin of the gastroduodenal, right gastric and cystic arteries. Any patient in this study was achieved pre-treatment coil embolization of non-target arteries. Sluggish flow of the tumor feeding arteries was suggestive of embolization endpoint. Any adverse event was evaluated and recorded according to Society of Interventional Radiology Clinical Practice Guidelines (SIR). The definition of the major complication was event that if left untreated might threaten the patient's life, lead to substantial morbidity and disability, or result in hospital admission or substantially lengthened hospital stay. The rest of the complications were classified as minor[12].

Follow up protocol and outcome evaluation

Assessment of tumor response following DEB-TACE by multiphase CT or MRI was scheduled 4 weeks following DEB-TACE and every 3 months after that. If residual viable tumor was depicted, repeated embolization was performed 2-4 weeks after follow up imaging. Other optional treatment modalities (conventional TACE, radiofrequency ablation, surgical resection) were considered if residual viable tumor deemed unsuitable for DEB-TACE.

The follow up imaging was classified according to EASL criteria. The EASL acknowledges "viable areas" as those that "present enhancement" and "necrotic areas" as those that "absent enhancement". According to the EASL criteria, complete response (CR) is described as neither viable tumor nor new lesion demonstrated (Figure 2); partial response (PR)

when a 50% reduction in viable tumor is depicted (Figure 3); stable disease (SD) in all other cases and progressive disease (PD) when either 25% escalating viable tumor or new lesion present. Objective response (OR) comprised both complete and partial response[5]. The complications developed within 4 weeks after embolization were considered as procedure-related complication.

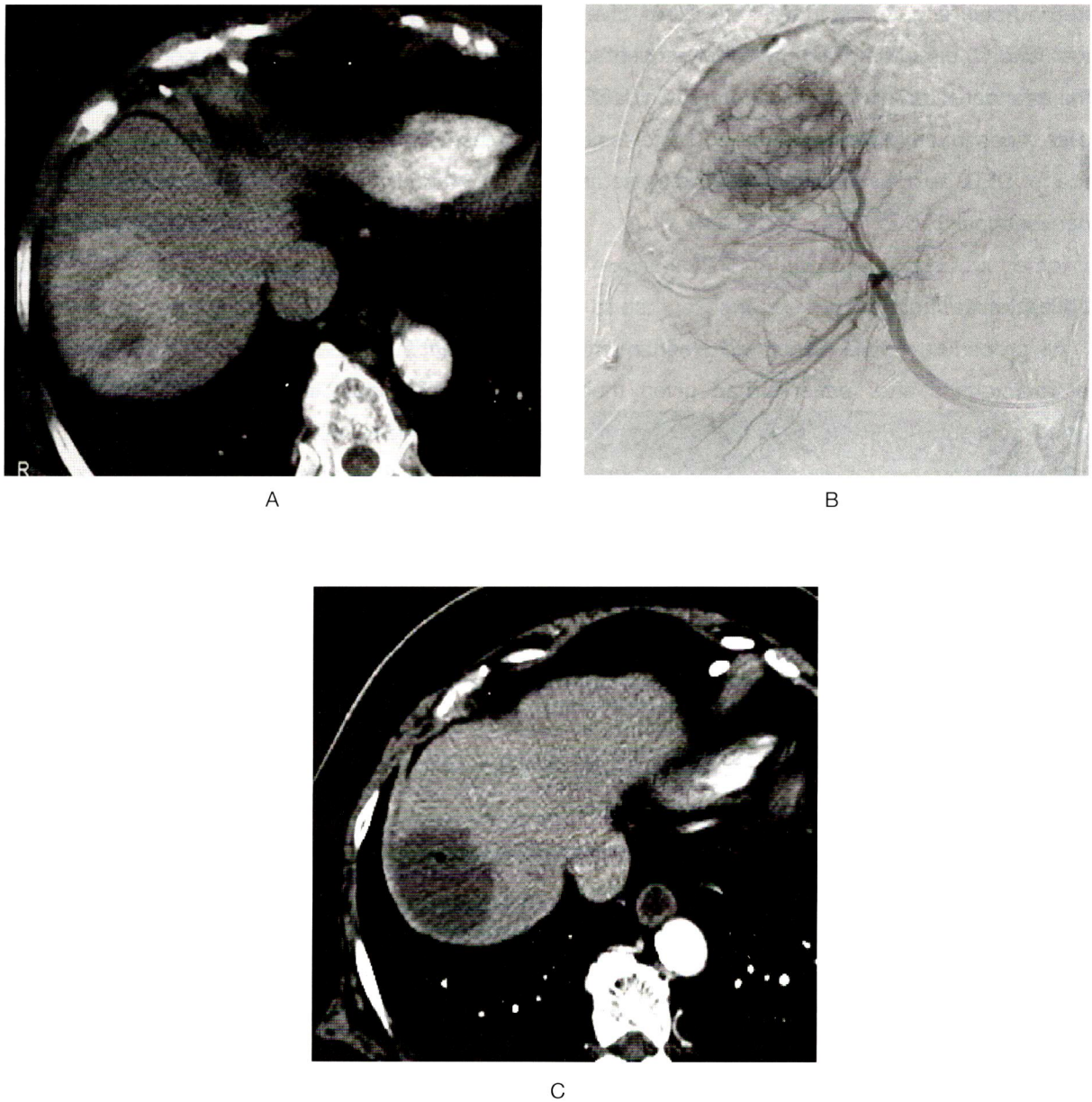

Fig.2 A 74-year old female with single HCC, feed by replaced RHA (A&B). Follow CT for one month showed CR after the 1st DEB-TACE (C).

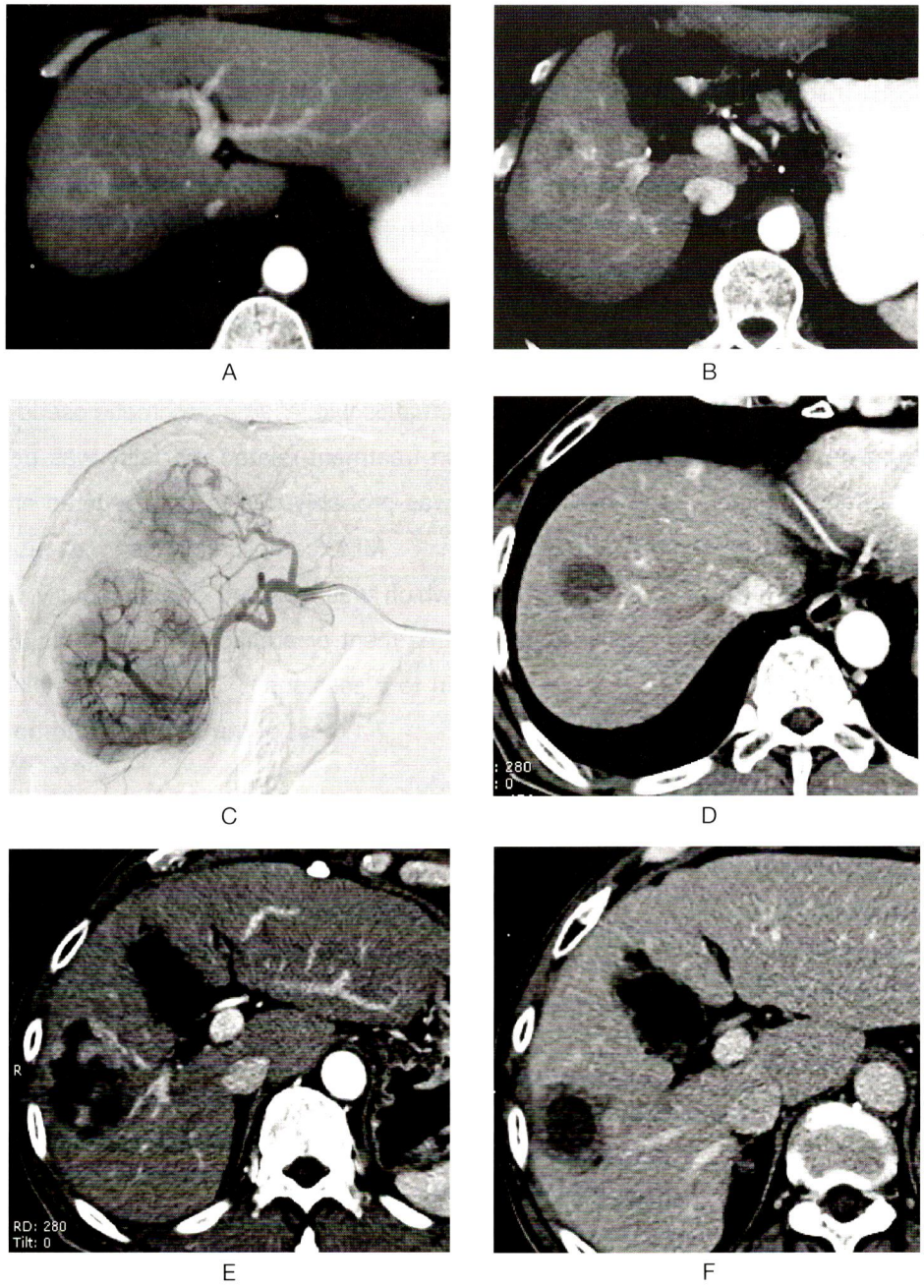

Fig.3 A 70-year-old male with two HCCs

A: Smaller one has single feeder from MHA.

B: The larger one feed by MHA & RHA.

C: Two hypervascular masses at right lobe liver.

D&E: Follow CT after 1st DEB-TACE showed CR of the smaller one and PR of the larger one.

F&G: Follow CT after 3rd DEB-TACE showed CR of the larger one with intratumoral air and sclerosing cholangitis

Statistical analysis

Fishers exact test was conducted to evaluate variables in this study. The differences at $p < 0.05$ were considered significant. Statistical analysis was performed using STATA (StataCorp LP, Texas, USA).

Results

Patients

Table 1 presents baseline characteristics of 10 patients (8 male and 2 female) included in this study. Seven patients (70%) presented with Child-Pugh A and 3 (30%) with Child-Pugh B. Seven patients (70%) had hepatitis, 5 had hepatitis B and 4 had hepatitis C.

Seven of 10 patients (70%) presented with single tumor while the other three patients had two tumors each. Total number of the lesions was 13 and the mean tumor diameter was 4.1 cm.

Of these 13 lesions, eight (61.53%) were smaller than 5 cm and 5 (38.46%) were larger than 5 cm. Eight of them (61.5%) had single feeding artery.

Procedure

A total of 16 embolization sessions were performed in 10 patients. Six patients had received one session, two had received two sessions and the remaining two had received three sessions. One patient in this study dropped out after the 1st follow up.

Tumor response

Of 13 HCCs, eight lesions were completed after the first session, one lesion after the second sessions and two lesions after the third sessions. No recurrence of disease was detected within 3 months after complete response (Table 2).

All eight lesions, which were completely responsive after the 1st session, had single arterial feeder ($p < 0.001$). Most of them (87.5%) were smaller than 5 cm in size ($p < 0.032$).

Adverse effect and complication

Unfortunately, one severe necrotizing pancreatitis with a large pancreatic pseudocyst resulting in treatment-related mortality was detected, which was probably due to non-targeted embolization.

Mild complication seen as abdominal pain, which was resolved spontaneously without further treatment or additional hospital stay, was detected in four sessions.

The rest of the sessions had no complication.

Disscussion

TACE is an effective option for patients with inoperable HCC. Survival improvement is due to the achievement of a treatment response reflected by extensive tumor necrosis. The high affinity for doxorubin and the slow-release mechanism are unique properties of DEB that were not observed with other commercially available embolization agents[7]. DEB-TACE is new tool, achieving major tumor necrosis and longer duration of the antitumoral agent while reducing side effect of the chemotherapy. Doxorubicin level in the peripheral blood of DEB TACE was significantly lower than conventional TACE[9].

In this study, the authors depicted good complete response in 11 lesions (91.66%) and 8 of these (61.53%) were completely necrotic after the 1st session (Table 2). The number of the embolization session in the patient treated with DEB-TACE is slightly lower than conventional TACE[12]. Average

Table 1 Baseline characteristics of 10 patients included in this study.

Characteristics	
Age	
Mean	66.9
Range	51-80 yrs old
Sex	
M	8
F	2
Hepatitis	7
Child Pugh	
A	7
B	3
Number of lesions	1.3 (1-2)
Number longest diameter	
Mean	4.1 cm
Range	0.5-8.8 cm
Number lesions	
Size < 5 cm	8 (61.53%)
Size > 5 cm	5 (38.46%)
Feeder	
Single feeder	8 (61.53%)
Multiple feeders	5 (38.5%)
Procedure per patient	1.6 (1-3)
Procedure per tumor	1.5 (1-3)

Table 2 Tumor response

Outcome	1st follow up	2nd follow up	3rd follow up
CR	8/13 (61.53%)	9/13 (69.23%)	11/12 (91.66%)
PR	2/13 (15.38%)	3/13 (23.07%)	0
SD	3/13 (23.07%)	0	1/12 (8.33%)
PD	0	0	0
OR	10/13 (76.92%)	12/13 (92.30%)	11/12 (91.66%)
Death	0	0	1
Loss FU	0	1	1

number of the embolization session in the patient is approximately 1.6 sessions and this seems to be a favorable result even though no controlled group of conventional TACE was performed.

In this study, the lesions were classified into two groups according to baseline tumor size and feeding artery. Among the tumors that were smaller than 5 cm, good complete response after the 1st session was achieved with significant difference as compared with the lesion larger than 5 cm ($p < 0.032$). The author also depicted significant difference of the complete response after the 1st session between single feeding artery and multiple feeding arteries. The larger the tumor size, the less possibility of complete necrosis in one session of embolization probably explained the reasons supporting these results. Another possible reason could be collateral supply from multiple feeding arteries limiting

Table 3 Factor predicting CR in 1st session

Factor	p-value
Sex	1.00
Child Pugh	1.00
Hepatitis B	0.592
Hepatitis C	0.105
Tumor size	0.032
Single feeding artery	0.001

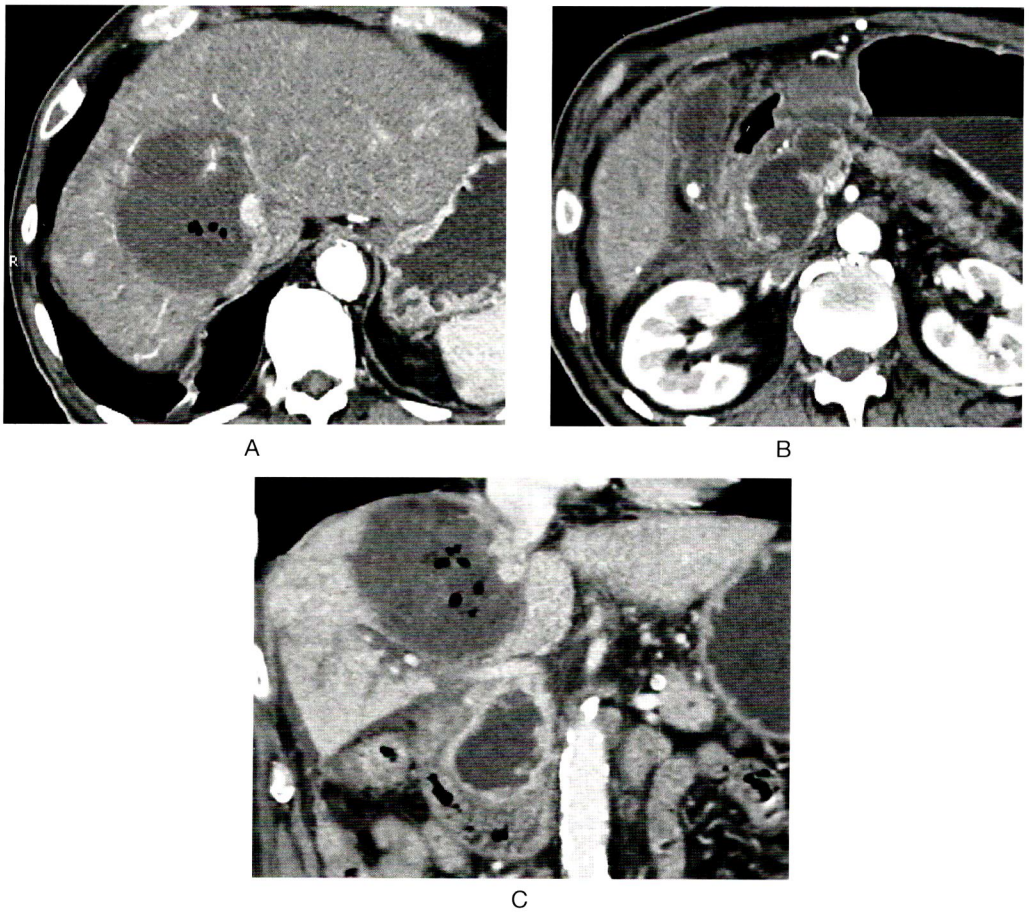

Fig.4 A 75-year-old male with HCC
A: Follow CT 1 month after 2nd TACE showed PR of the HCC with intratumoral air bubbles.
B&C: A large pancreatic pseudocyst with surrounding inflammation.

Table 4 Complication Rate

Complication	Number	Percentage
No	11/16	68.75
Mild	4/16	25
Moderate	0	0
Severe	1/16	6.25

complete necrosis (Table 3).

As with the previous DEB-TACE studies, no systemic toxicity from Doxorubicin was demonstrated in this study[13,14]. The incidence of serious treatment related complication and treatment related death following conventional TACE has been reported to be 27.5% and 9.5% respectively[15,16]. O Nawawi et al. reported the treatment-related complication and treatment- related death following DEB-TACE were 21.2% and 10.5% respectively. The incidence of the mild complication in this series is 25% per procedure, representing as abdominal pain. Only one patient had severe complication, severe necrotizing pancreatitis with a large pancreatic pseudocyst, leading to 10% of treatment-related death (Figure 4) (Table 4). The proposed mechanism of the pancreatitis following TACE is inadvertent embolization through collateral vessels or regurgitation of the embolic material to non-targeted arteries[17,18]. Prophylactic embolization of non-target arteries may be taken in the cases where superselective injection is not possible.

The overall limited number of patients included in this study caused limitation as well as being a retrospective study and short follow-up. Randomized controlled trial prospective study should overcome this limitation.

In conclusion, TACE with DEB had good successful rate for inoperable HCC with mild complication. Tumor size smaller than 5 cm and single tumor arterial feeder were significant factors influencing successful rate.

References

1. Jemal A, Bray F, Center MM, Ferlay J, Ward E, Forman D. Global cancer statistics. CA Cancer J Clin 2011 Mar-Apr;61(2):69-90.
2. Omata M, Lesmana LA, Tateishi R, Chen PJ, Lin SM, Yoshida H, et al. Asian Pacific Association for the Study of the Liver consensus recommendations on hepatocellular carcinoma. Hepatol Int 2010;4(2):439-74.
3. Yamada R, Sato M, Kawabata M, Nakatsuka H, Nakamura K, Takashima S. Hepatic artery embolization in 120 patients with unresectable hepatoma. Radiology 1983 Aug;148(2): 397-401.
4. Ramsey DE, Kernagis LY, Soulen MC, Geschwind JF. Chemoembolization of hepatocellular carcinoma. J Vasc Interv Radiol 2002 Sep;13(9 Pt 2):S211-21.
5. Nawawi O, Hazman M, Abdullah B, Vijayananthan A, Manikam J, Mahadeva S, et al. Transarterial embolisation of hepatocellular carcinoma with doxorubicin-eluting beads: single centre early experience. Biomed Imaging Interv J 2010 Jan;6(1):e7.
6. Malagari K. Drug-eluting Beads in the Treatment of Cirrhosis-related Hepatocellular Carcinoma. European Oncological Disease 2007;1(1):50-3.
7. Lewis AL, Gonzalez MV, Lloyd AW, Hall B, Tang Y, Willis SL, et al. DC bead: in vitro characterization of a drug-

delivery device for transarterial chemoembolization. J Vasc Interv Radiol 2006 Feb;17(2 Pt 1):335-42.

8. Hong K, Khwaja A, Liapi E, Torbenson MS, Georgiades CS, Geschwind JF. New intra-arterial drug delivery system for the treatment of liver cancer: preclinical assessment in a rabbit model of liver cancer. Clin Cancer Res 2006 Apr 15;12(8):2563-7.
9. Varela M, Real MI, Burrel M, Forner A, Sala M, Brunet M, et al. Chemoembolization of hepatocellular carcinoma with drug eluting beads: efficacy and doxorubicin pharmacokinetics. J Hepatol 2007 Mar;46(3):474-81.
10. Bruix J, Sherman M. Practice Guideline Committee, American Association for the Study of Liver Disease. Management of Hepatocellular Carcinoma: An Update. Hepatology 2010;53:1020-2.
11. Raoul JL, Heresbach D, Bretagne JF, Ferrer DB, Duvauferrier R, Bourguet P, et al. Chemoembolization of hepatocellular carcinomas. A study of the biodistribution and pharmacokinetics of doxorubicin. Cancer 1992 Aug 1;70(3):585-90.
12. Sacco R, Bargellini I, Bertini M, Bozzi E, Romano A, Petruzzi P, et al. Conventional versus doxorubicin-eluting bead transarterial chemoembolization for hepatocellular carcinoma. J Vasc Interv Radiol 2011 Nov;22(11):1545-52.
13. Lammer J. Clinical experience with drug eluting bead (DC Bead) for chemoembolisation of unresectable hepatocellular carcinoma. Data presentation at CIRSE; Nice, France 2005.
14. Poon R. Treatment of Asian patients with hepatocellular carcinoma (HCC) using doxorubicin eluting beads embolization (PRECISION ASIA Study). Presentation at CIRSE 2004; Barcelona 25-29 September 2004.
15. Llovet JM, Real MI, Montana X, Planas R, Coll S, Aponte J, et al. Arterial embolisation or chemoembolisation versus symptomatic treatment in patients with unresectable hepatocellular carcinoma: a randomised controlled trial. Lancet 2002 May 18;359(9319):1734-9.
16. Pelletier G, Ducreux M, Gay F, Luboinski M, Hagege H, Dao T, et al. Treatment of unresectable hepatocellular carcinoma with lipiodol chemoembolization: a multicenter randomized trial. Groupe CHC. J Hepatol 1998 Jul;29(1): 129-34.
17. Xia J, Ren Z, Ye S, Sharma D, Lin Z, Gan Y, et al. Study of severe and rare complications of transarterial chemoembolization (TACE) for liver cancer. Eur J Radiol 2006 Sep;59(3):407-12.
18. Leung TK, Lee CM, Chen HC. Anatomic and technical skill factor of gastroduodenal complication in post-transarterial embolization for hepatocellular carcinoma: a retrospective study of 280 cases. World J Gastroenterol 2005 Mar 14;11(10):1554-7.

THE ASEAN JOURNAL OF RADIOLOGY 2012: 18(2): 133-136 133

Case Report

Unusual-presenting Appendicitis Resulted From Hidden Location : A Case Report

Sornsupha Limchareon[1], Krisada Pojanasuwanchai[2]

[1] *Department of Radiology, Faculty of Medicine, Burapha University, Chonburi, Thailand*

[2] *Department of Surgery, Phyathai-Sriracha Hospital, Chonburi, Thailand*

Abstract

Acute appendicitis is a common clinical problem in emergency department. The clinical diagnosis of acute appendicitis may be straightforward for patients who present with classic signs and symptoms. However atypical presentations exist and may lead to diagnosis confusion and treatment delay. There are various causes of atypical presentations. Anatomic hidden location is one of the causes. We present a case of unusual-presenting appendicitis resulted from hidden location. It is the post-ileal typed appendix which only its distal-half is covered by peritoneum.

Introduction

The diagnosis of acute appendicitis is not always clear clinically because the classic signs and symptoms are found about 50%-60% of cases[1]. There have been reports of many unusual presentations of acute appendicitis[2-7]. Guidry et al. reported the anatomical "hidden" locations which caused acute appendicitis difficult to be diagnosed[8]. The hidden locations are including retroperitoneal, retroileal, and retrocecal/retrocolic positions[8]. This report is of a patient with delayed diagnosis of acute appendicitis because the retroileal-typed appendix lied partially in intra-peritoneum and partially in retroperitoneum.

Case Report

A 35-year-old woman presented to outpatient department because of pelvic pain, vomiting and low grade fever. She had had dysuria one week earlier. Physical examination was unremarkable. The laboratory findings revealed elevated white blood count (WBC 15,900, N 70%) and microscopic leucouria (WBC 3-5/HPF, leucocyte 3+). An ultrasound of the abdomen as well as transvaginal ultrasound were normal. Acute pyelonephritis was diagnosed and the patient was received intravenous antibiotic. The fever and vomiting had gone the next day. She was discharged two days after admission.

One week later, she was re-admitted because of continuation of the pelvic pain. Physical examination revealed tenderness and guarding at pelvic region. Laboratory results showed no leukocytosis and normal urine analysis. Ultrasound of the abdomen was normal. A computerized scan of the abdomen with intravenous contrast media showed irregular thickening of the appendiceal wall, only at distal-half which lied deep to the ileum in right sided pelvic cavity (Fig 1). Additional focused ultrasound demonstrated normal appearance of the proximal-half of the appendix while the distal-half was irregular thickening and hypoechoic wall associated with periappendiceal fat inflammation (Fig 2).

An appendectomy was performed. Operative finding revealed marked inflammation and adhesion over distal-half of the appendix. The appendix was post-ileal type with its distal-half covered by the peritoneum. Histologic examination of the appendix showed acute suppurative appendicitis with periappendicitis. She had uneventful recovery and was discharged. For the following two weeks, the patient was asymptomatic.

Discussion

Acute appendicitis is one of the most common causes of acute abdominal pain that required surgery. Accurate and prompt diagnosis is essential to minimized morbidity as major complications can occur when treatment is delayed. Classic symptoms of appendix start from poorly localized periumbilical

Fig.1 CECT revealed irregular thickening of distal appendiceal wall with periappendiceal fat stranding

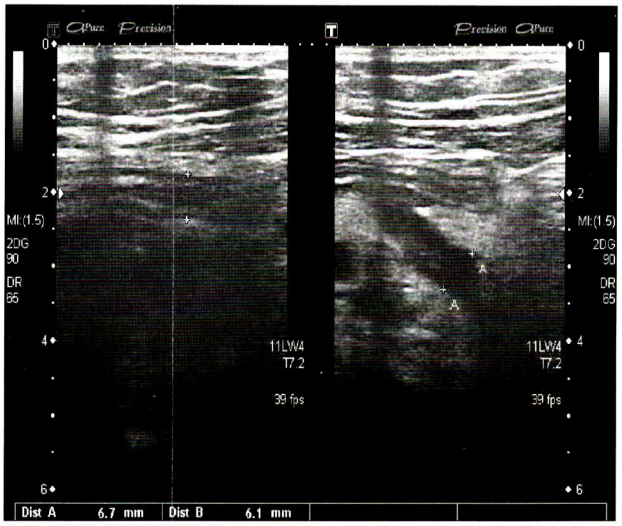

Fig.2 Focused ultrasound showed normal proximal appendix. The distal appendix revealed irregular thickening and hypoechoic wall with periapppendiceal fat inflammation.

pain, followed by nausea and vomiting. Patients may be afebrile or have a low-grade fever. Subsequently the pain migrates to right lower quadrant. Physical findings vary with time and with the locations of appendix[8,9]. The classic presentation occurs in only 50%-60% of patients[1]. Thus atypical presentation is not uncommon. Among various causes of atypical-presenting appendicitis, hidden location is one of these causes[8]. Atypical presentations may result in delayed or missed diagnosis as occurred in our patient.

Position of the appendix has been described as retrocecal, pelvic, postileal, paracecal/ subcecal and preileal. Most literature found retrocecal position is the most common type[9-12]. A few reports presented pelvic position is more common[13] especially in younger age[11]. The appendix is reported to be "hidden" in a retroperitoneal, retroileal, retrocecal or retrocolic location[8]. To the best of our knowledge, there has been no prior report of retroileal-typed appendix which partially lied in retro-peritoneum. This could irritate the right ureter and cause urinary frequency in our patient. However Chin-San et al found that small amount of WBC in urine (3-5 cells/ HPF) showed no statistical difference between simple acute appendicitis patients and normal patients[14].

Ultrasound is usually used as a first imaging modality especially in women of child-bearing age. The overall accuracy of ultrasound in diagnosis of acute appendicitis is approximately 80%[1] and as high as 94% in the report by Rioux M[15]. The appendix of our patient is deep retroileal location, resulting in false negative ultrasound on both admissions.

Helical CT has become a primary imaging modality in patients with suspected appendicitis because of its high accuracy[16-21]. Coursey CA, et al. concluded that pre-operative CT in the evaluation of women under 45 years of age who suspected of having acute appendicitis is associated with a lower negative appendectomy rate[17]. CT findings in acute appendicitis are including ; appendiceal enlargement, appendiceal wall thickening, periappendiceal fat stranding and appendiceal wall enhancement[22]. Omar et al. recommened to use abdominal CT scan for all patients in whom the diagnosis of acute appendicitis is considered[20].

Conclusion

We present a rare position of the appendix which is retroileal-type, partly-lied in intra-peritoneum and partly in retroperitoneum. This hidden location resulted in unusual presentation and missed diagnosis initially. CT scan is of diagnostic value is unusual-presenting appendicitis.

Acknowledgements

We wish to thank Dr.Chanchai Leesomprasong, Medical Director of Phyathai Sriracha Hospital from his support, Dr.Somchai Youngsiri and Dr.Alisara Wongsuttilert for their helpful assistance.

References

1. Saddique M, Iqbal P, Rajput A, Kumar R. Atypical presentation of appendicitis: diagnosis and management. JSP 2009 Oct-Dec;14(4):157-60.
2. Giuliano V, Giuliano C, Pinto F, Scaglione M. Chronic appendicitis "syndrome" manifested by an appendicolith and thickened appendix presenting as chronic right lower quadrant pain in adults. Emerg Radiol 2006 Mar;12:96-8.
3. Sheikh IA, Hanif MS. Recurrent acute/chronic appendicitis an independent clinical entity. PAFMJ.2005 Dec;4(about 2 p).Available from:http:/www.pafmj.org/showdetails.php?id=71&t=0
4. Falk S, Schutze U, Guth, Stutte HJ. Chronic recurrent appendicitis. A clinicopathologic study of 47 cases. Eur J Pediatr Surg 1991 Oct;1(5):277-81.
5. Safaei M, Moeinei L, Rasti M. Recurrent abdominal pain and chronic appendicitis. J Res Med Sci 2004;1:11-4.
6. Gibeily GJ, Ross MN, Manning DB, Wherry DC, Kao TC. Late-presenting appendicitis. a laparoscopic approach to a complicated problem. Surg Endosc 2003 May;17(5):725-9.
7. Andiran F, Dayi S, Caydere M, Ustun H. Chronic recurrent appendicitis in children: an insidious and neglected cause of surgical abdomen. Turk J Med Sci 2002;32:351-4.
8. Guidry SP, Poole GV. The anatomy of appendicitis. Am Surg 1994 Jan;60(1):68-71.
9. Ali U, Noor A, Jan WA, Islam M, Khan AS, Khan M. Anatomical position of appendix in emergency care patients. J Postgrad Med Inst 2010;24(3):207-11.
10. Paul UK, Naushaba H, Begum T, Alam MJ, Alim AJ, Akther J. Position of vermiform appendix: a postmortem study. Bangladesh J. Anat 2009 Jan;77(1):34-6.
11. Iqbal T, Amanullah A, Nawaz R. Pattern and positions of vermiform appendix in people of Bannu district. GJMS 2012 Jan-Jun;10(1):100-3.
12. Clegg-Lamptey JN, Armah H, Naaeder SB, Adu-Aryee NA. Position and susceptibility to inflammation of vermiform appendix in Accra, Ghana. East Afr Med J 2006 Dec;83(12):670-3.
13. Golalipour MJ, Arya B, Azarhoosh R, Jahanshahi M. Anatomical variations of vermiform appendix in South-East Caspian Sea (Gorgan-IRAN). J Anat. Soc. India 2003;52 (2):141-3.
14. Wei CS, Wu HP, Chang YJ. Routine urine analysis in patients with acute appendicitis. J Emerg Crit Care Med 2007;18(2):71-8.
15. Rioux M. Sonographic detection of the normal and abnormal appendix. AJR Am J Roentgenol 1992 Apr; 158(4): 773-8.
16. Nikolidis P, Hwang CM, Miller FH, Papanicolaou N. The non visualized appendix: incidence of acute appendicitis when secondary inflammatory changes are absent. AJR Am J Roengenol 2004 Oct;183(4):889-92.
17. Coursey CA, Nelson RC, Patel MB, Cochran C, Dodd LG, Delong DM, et al. Making the diagnosis of acute appendicitis: do more preoperative CT scans mean fewer negative appendectomies? A 10-year study. Radiology 2010 Feb;254(2):460-8.
18. Choi YH, Fischer E, Hoda SA, Rubenstein WA, Morrissey KP, Hertford D, et al. Appendiceal CT in 140 cases. Diagnostic criteria for acute and necrotizing appendicitis. Clinical Imaging 1998 Jul-Aug;22(4):252-71.
19. Raman SS, Lu DS, Kadell BM, Vodopich DJ, Sayre J, Cryer H. Accuracy of non-focused helical CT for the diagnosis of acute appendicitis: a 5-year review. AJR Am J Roengenol 2002 Jun;178(6):1319-25.
20. Llaguna OH, Avgerinos D, Cha A, Friedma R, Surick BG, Leitman IM. The impact of liberal use of CT in the work up of acute appendicitis. The Open Surgery journal 2009; 3:11-4.
21. Gwynn LK. The diagnosis of acute appendicitis: clinical assessment versus computed tomography evaluation. J Emerg Med 2001 Aug;21(2):119-23.
22. Choi D, Park H, Lee YR, Kook SH ,Kim SK, Kwag HJ, et al. The most useful findings for diagnosing acute appendicitis on contrast-enhanced helical CT. Acta Radiol 2003 Nov;44(6):574-82.